EUROPEAN ORGANIZATION FOR NUCLEAR RESEARCH (CERN)

CERN-EP-2026-001
2026/09/09

CMS-B2G-23-007

Search for heavy scalar resonances decaying to Lorentz-boosted Higgs and Higgs-like bosons in the $b\bar{b}4q$ final state at $\sqrt{s} = 13$ TeV

The CMS Collaboration*

arXiv:2602.00273v2 [hep-ex] 5 Sep 2026

Abstract

A search is performed for a heavy scalar resonance X decaying to a Higgs boson (H) and a Higgs-like scalar boson (Y) in the two bottom quark ($H \to b\bar{b}$) and four quark ($Y \to VV \to 4q$) final state, where V denotes a W or Z boson. Masses of the X between 900 and 4000 GeV and the Y between 60 and 2800 GeV are considered. The search is performed in data collected by the CMS experiment at the CERN LHC from proton-proton collisions at 13 TeV center-of-mass energy, with a data set corresponding to a total integrated luminosity of 138 fb^{-1}. It targets the Lorentz-boosted regime, in which the products of the $H \to b\bar{b}$ decay can be reconstructed as a single large-area jet, and those from the $Y \to VV \to 4q$ decay as either one $Y \to 4q$ or two $V \to q\bar{q}$ jets. Jet identification and mass reconstruction exploit machine-learning tools, including a novel attention-based "particle transformer" for $Y \to 4q$ identification. No significant excess is observed in the data above the standard model background expectation. Upper limits on the product of production cross section and branching fraction as low as 0.2 fb are derived at 95% confidence level for various mass hypotheses. This is the first search at the LHC for scalar resonances in the all-hadronic $b\bar{b}VV$ decay channel.

Published in the Journal of High Energy Physics as doi:10.1007/JHEP08(2026)050.

© 2026 CERN for the benefit of the CMS Collaboration. CC-BY-4.0 license

*See Appendix A for the list of collaboration members

1 Introduction

Many theoretical models predict a richer scalar sector than that of the standard model to address its foundational and observational inconsistencies, such as the Higgs boson (H) mass hierarchy problem and the baryon asymmetry in the universe. These include two-Higgs-doublet models [1] that add a scalar doublet to the standard model, such as the minimal supersymmetric extension of the standard model (MSSM) [2]. The MSSM predicts two neutral *CP*-even scalars (H_0, h), one neutral *CP*-odd scalar (A), and two charged scalars ($H^{\pm}$), where one of the neutral *CP*-even scalars may be the state observed at 125 GeV. The next-to-MSSM [3] adds to this a complex scalar singlet, predicting additional *CP*-even and *CP*-odd neutral scalars. Finally, the two-real-singlet model [4] predicts two additional *CP*-even scalar fields. Depending on the masses of the additional scalar particles, all of these models allow the decays of a heavier scalar to symmetric and asymmetric pairs of light scalars, such as HH and hH, respectively.

Motivated by these theoretical models, we search for decays of the form $X \to HY$, where X is the heavier and Y the lighter new scalar resonance, with H decaying to a bottom quark-antiquark pair, $b\bar{b}$, and Y to four quarks via $VV \to 4q$, where V denotes a W or Z boson. Many models, such as the two-real-singlet model, predict that the branching fractions of the lighter scalar boson to different standard model particles are similar to or the same as those of the standard model Higgs boson. Assuming the same mass-dependent branching fractions as the standard model Higgs boson [5], the WW and ZZ decay modes are dominant for masses of the Y boson $m_Y > 140$ GeV and, hence, the $H \to b\bar{b}$ and $Y \to VV$ decays will be the dominant signatures for the $X \to HY$ signal.

We target the high X mass (m_X) regime, in which the Higgs boson is highly Lorentz-boosted, with the $H \to b\bar{b}$ system reconstructed as a large-area jet. Two regimes are considered for the $Y \to VV$ decay: one where $m_Y \lesssim 0.1 m_X$, resulting in a highly boosted Y with its $VV \to 4q$ decay products merged and reconstructed as a single large-area jet ("fully merged"); and the second where $0.1 m_X \lesssim m_Y < m_X - m_H$, in which Y is not as boosted, and each daughter V is instead reconstructed individually as a large-area jet ("semimerged"). Schematic diagrams of the decays targeted in the two regimes are depicted in Fig. 1.

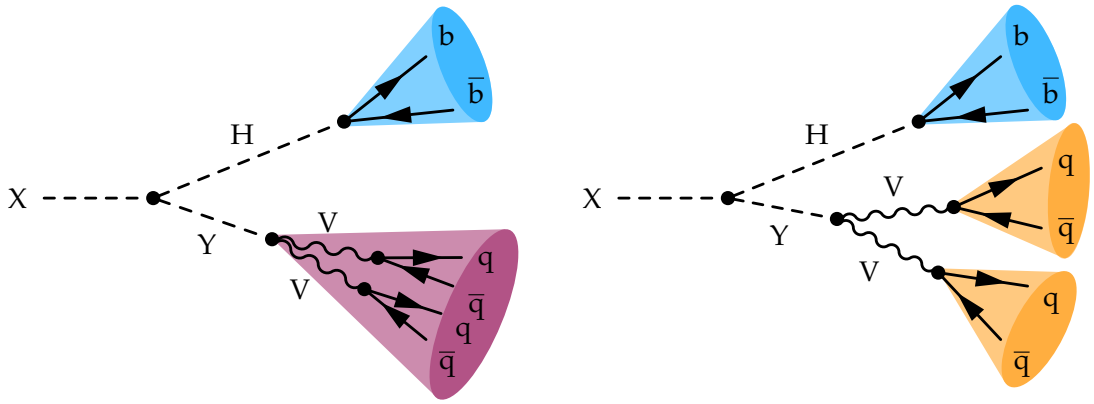

Figure 1: Schematic diagrams of the $X \to HY$ decay in the $H \to b\bar{b}$ and $Y \to VV \to 4q$ all-hadronic final state, with V = W or Z. Left: The fully merged regime ($m_Y \lesssim 0.1 m_X$) in which Y is highly boosted, with its decay products merged and reconstructed as a single large-area jet. Right: The semimerged regime ($0.1 m_X \lesssim m_Y < m_X - m_H$) in which Y is not as boosted, and each daughter V boson is instead reconstructed individually as a large-area jet.

There have been several searches for $X \to HY$ production in a variety of kinematic regimes and final states with the data collected by the CMS experiment at the CERN LHC between

2016–2018, such as the merged 4b final state [6] and the resolved $b\bar{b}\gamma\gamma$ [7] and $b\bar{b}\tau\tau$ [8] final states. Similarly, ATLAS has searched for this process in the $\gamma\gamma b\bar{b}$ [9] final state, along with the $\gamma\gamma VV$ [10] and $\tau\tau VV$ [11] final states. Previous searches at CMS in the $b\bar{b}VV$ final state have only been conducted in symmetric decays of the form $X \to HH$ [12], and only in the semileptonic channel.

In this paper, we present the first search for asymmetric cascade decays of the form $X \to HY$ in the all-hadronic $b\bar{b}VV$ final state. The analysis is performed using data collected by CMS from proton-proton (pp) collisions at $\sqrt{s} = 13\,\text{TeV}$ in 2016–2018, with a data set corresponding to a total integrated luminosity of $138\,\text{fb}^{-1}$ [13, 14].

The paper is organized as follows. Section 2 provides a brief overview of the CMS detector. Section 3 describes the simulated samples used in this analysis, followed by a description of the event reconstruction and techniques used to improve the jet mass resolution in Section 4. The event selection and object identification criteria for the fully merged and semimerged categories are outlined in Section 5. A description of the background estimation method and its validation is provided in Section 6. Section 7 summarizes the sources of systematic uncertainty in the analysis. Finally, the results are presented in Section 8 and summarized in Section 9. Tabulated results are presented in the HEPData record for this analysis [15].

2 The CMS detector

The central feature of the CMS apparatus is a superconducting solenoid of 6 m internal diameter, providing a magnetic field of 3.8 T. Within the solenoid volume are a silicon pixel and strip tracker, a lead tungstate crystal electromagnetic calorimeter (ECAL), and a brass and scintillator hadron calorimeter (HCAL), each composed of a barrel and two endcap sections. Forward calorimeters extend the pseudorapidity (η) coverage provided by the barrel and endcap detectors. Muons are reconstructed using gas-ionization detectors interleaved with the layers of the steel flux-return yoke outside the solenoid. More detailed descriptions of the CMS detector, together with a definition of the coordinate system used and the relevant kinematic variables, can be found in Refs. [16, 17].

Events of interest are selected using a two-tiered trigger system. The first level, composed of custom hardware processors, uses information from the calorimeters and muon detectors to select events at a rate of around 100 kHz within a fixed latency of $4\,\mu$s [18]. The second level, known as the high-level trigger, consists of a farm of processors running a version of the full event reconstruction software optimized for fast processing, and reduces the event rate to a few kHz before data storage [19, 20].

3 Event simulation

The $X \to HY$ signal samples are simulated via gluon fusion at leading order in the 900–4000 GeV m_X range and 60–2800 GeV m_Y range, with widths of 1 MeV each, using the MADGRAPH5_aMC@NLO 2.6.5 [21] event generator. The $H \to b\bar{b}$ and $Y \to WW \to 4q$ decays are simulated with PYTHIA (v8.205) [22]. Signal samples are produced in the next-to-MSSM with the narrow-width approximation, which allows for the interpretation of the results in the context of other scenarios beyond the standard model under the same approximation. The simulation of parton showering, underlying event interactions, and hadronization is performed with PYTHIA (v8.205), including parameters from the CP5 tune [23].

The primary background is composed of jets produced through the strong interaction, referred to as quantum chromodynamics (QCD) multijet events. It is simulated with two to four jets in the final state and at leading order with MADGRAPH5_aMC@NLO 2.2.2, though it is estimated primarily via control samples in data. Minor backgrounds include top quark (t) events, such as $\mathrm{t\bar{t}}$+jets and single t+jets, which are simulated with POWHEG 2.0 [24–28] and PYTHIA 8; V+jets and diboson events, simulated with MADGRAPH5_aMC@NLO and PYTHIA 8; and standard model H events, dominated by associated production with a V boson and simulated with POWHEG 2.0 and PYTHIA 8. All simulated samples are generated with the NNPDF 3.0 [29] or 3.1 [30] parton distribution functions (PDFs). The response of the CMS detector is modeled with the GEANT4 [31] package, with additional simulated pp interactions superimposed on the hard interactions in simulated events to model pileup effects. The distribution of the number of pileup interactions in the simulation is reweighted to match the corresponding distribution in data, which is obtained using the measured instantaneous luminosity per bunch crossing.

4 Event reconstruction

A particle-flow algorithm [32] aims to reconstruct and identify each individual particle in an event, with an optimized combination of information from the various elements of the CMS detector. The energy of photons is obtained from the ECAL measurement. The energy of electrons is determined from a combination of the electron momentum at the primary interaction vertex as determined by the tracker, the energy of the corresponding ECAL cluster, and the energy sum of all bremsstrahlung photons spatially compatible with originating from the electron track. The energy of muons is obtained from the curvature of the corresponding track. The energy of charged hadrons is determined from a combination of their momentum measured in the tracker and the matching ECAL and HCAL energy deposits, corrected for the response function of the calorimeters to hadronic showers. Finally, the energy of neutral hadrons is obtained from the corresponding corrected ECAL and HCAL energies. The primary vertex is taken to be the vertex corresponding to the hardest scattering in the event, evaluated using tracking information alone, as described in Section 9.4.1 of Ref. [33].

For each event, hadronic jets are clustered from these reconstructed particles using the infrared- and collinear-safe anti-k_{T} algorithm [34, 35] with a distance parameter of 0.8 (AK8 jets). Jet momentum is determined as the vectorial sum of all particle momenta in the jet, and is found from simulation to be, on average, within 5 to 10% of the generator jet momentum over the entire transverse momentum (p_{T}) spectrum and detector acceptance [36]. Additional pp interactions within the same or nearby bunch crossings (pileup) can contribute additional tracks and calorimetric energy depositions to the jet momentum. The pileup-per-particle identification algorithm [37] is used to mitigate the effect of pileup at the reconstructed particle level, making use of local shape information, event pileup properties, and tracking information. Additional selection criteria are applied to each jet to remove those potentially dominated by instrumental effects or reconstruction failures. A comprehensive description of these criteria and the full jet momentum calibration procedure is provided in Ref. [38].

Jet mass is reconstructed by different algorithms, depending on the type of jet and context. In the high-level trigger, the "trimmed mass" is defined as the invariant mass of the jet constituents after a jet trimming procedure [39] to remove soft and wide-angle radiation, using a subjet size parameter of 0.3 and a subjet to AK8 jet p_{T} fraction of 0.1. Offline, a mass regression algorithm is employed, which uses the PARTICLENET architecture [40, 41], leveraging particle-flow candidate and secondary vertex information in a graph neural network to predict the "regressed jet mass" (m_{reg}) [42]. The PARTICLENET model has demonstrated improved mass

resolution for AK8 jets by up to 10% compared to alternative algorithms [42].

5 Event selection

The online selection consists of triggers requiring events with a scalar sum of jet transverse momenta, H_T, of at least 800, 900, or 1050 GeV, depending on the data-taking period. Further trigger selection records events with at least one AK8 jet with a $p_T \geq 400$ or 500 GeV, where in the case of the former, an additional requirement that the jet has a trimmed mass of at least 40 GeV is imposed. Finally, triggers requiring an H_T of 750 or 800 GeV with all jets having trimmed masses of at least 50 GeV are also used to target the boosted, fully hadronic nature of the final state. The efficiency for the combined set of triggers is measured in data in a sample composed primarily of AK8 jets originating from hadronically decaying top quarks, as a function of jet p_T and mass, and is applied to simulated background and signal processes. The signal efficiency of the online selection ranges from 90% for low $m_X \approx 1000$ GeV to close to 100% for higher $m_X \gtrsim 1500$ GeV.

The $H \to b\bar{b}$ decay is targeted through an offline selection for a single AK8 jet, while the $Y \to VV$ decay is selected as either one or two AK8 jets, in the fully merged and semimerged categories, respectively. In both cases, PARTICLENET is used to discriminate signal $H \to b\bar{b}$ jets from QCD background using a discriminant T_{Xbb} derived from its outputs. These outputs have been decorrelated from the jet masses by enforcing a uniform distribution in jet mass and p_T in the training samples [43]. Three T_{Xbb} working points (WPs, adjusted for each data-taking year [41]) are considered in the analysis: "low", "medium", and "high" purity (LP, MP, and HP), corresponding to signal (QCD background) efficiencies of approximately 80 (0.8), 60 (0.3), and 40 (0.1)%, respectively. An overview of the training, mass decorrelation, and calibration of the PARTICLENET $H \to b\bar{b}$ tagger can be found in Ref. [41]. As jet mass resolution is crucial to the sensitivity of the search, the regressed mass observable m_{reg} is used for all AK8 jets.

The V bosons in the simulated $Y \to VV$ samples, used to train the jet classification algorithms for both the fully merged and semimerged categories of events, are W bosons that decay hadronically. As a result, the sensitivity to the $Y \to ZZ$ decay mode is less than that for $Y \to WW$. The selection efficiency for signals with the $Y \to ZZ$ decay is measured in a subset of signal samples to be a factor of 0.73 and 0.78 times that of WW decays in the fully merged and semimerged categories, respectively.

For both categories, a "signal pass" (SP) region is optimized for performing the search. An independent "signal fail" (SF) region with the tagger selections inverted is also used as a control region to estimate the QCD multijet background, as described in Section 6. Along with these signal regions (SRs), which require the $b\bar{b}$ candidate m_{reg} (m^{bb}_{reg}) to be within a window around m_H, we define validation pass (VP) and validation fail (VF) regions by the sidebands of this mass window to validate the background estimation method before observing data in the SRs. These validation regions (VRs) are used purely to confirm the agreement of the background model with data and are not used in the final search. Signal contamination in the VRs and the SF region is $<1\%$ for both the fully merged and semimerged categories, assuming signal cross sections corresponding approximately to those obtained from scans of the next-to-MSSM benchmark planes across the range of m_X and m_Y considered in Ref. [44]. Detailed selections for all four regions for both categories are defined below with a schematic of the event categorization provided in Fig. 2.

5.1 Fully merged category

For $m_Y \lesssim 0.1 m_X$, the fraction of signal $Y \to VV$ AK8 jets containing four quarks is approximately 80–90%, and decreases to around 40% in the region $0.1 m_X \lesssim m_Y \lesssim 0.16 m_X$ before rapidly dropping off. Thus, in the case where $m_Y \lesssim 0.1 m_X$, both V bosons and at least three out of four of their combined quark decay products are assumed to be reconstructed as a single AK8 jet. Hence, selected events are required to have at least two AK8 jets with $|\eta| < 2.4$, corresponding to the Higgs and Y boson candidates. The leading and subleading (in p_T) jets are required to have $p_T > 400$ and 350 GeV, respectively. Out of all AK8 jets in the event passing these requirements, the one with the highest T_{Xbb} score is then considered as the $H \to b\bar{b}$ candidate jet, and is required to pass the HP WP of the tagger. This $b\bar{b}$ candidate jet is also required to have a jet mass close to m_H: $110 < m_{reg} < 145$ GeV.

To identify the $Y \to VV \to 4q$ jet, we employ an attention-based neural network, referred to as "particle transformer" (PART) [45], which is trained on jets originating from scalar H-like resonances decaying to WW, with at least one W boson decaying hadronically [46].

The PART algorithm is decorrelated with the jet mass by enforcing a uniform distribution in jet mass, and by varying the masses of the daughter V bosons such that the ratio of V and Y boson masses at each m_Y point is equal to the ratio of V and Higgs boson masses in the standard model [46]. Because the mass of the scalar resonance in the training samples only varies between 15–250 GeV, the selection efficiency for signal jets with m_Y exceeding this range is lower by a factor of three compared to those with m_Y within this range. A detailed description of the training, mass decorrelation, and performance of this network is provided in Ref. [46].

The outputs of PART are used to derive the T_{YWW} discriminant, isolating the $Y \to VV$ signal from QCD and t background jets, defined as:

$$T_{YWW} = \frac{P_{HWW4q} + P_{HWW3q}}{P_{QCD} + P_{top} + P_{HWW4q} + P_{HWW3q}}, \tag{1}$$

where P_{HWW4q}, P_{HWW3q}, P_{QCD}, and P_{top} are the predicted probabilities of the jet being a four-pronged VV-jet, three-pronged VV-jet, QCD jet, or t jet, respectively. The AK8 jet with the highest T_{YWW} score that also passes the above p_T and η kinematic selections is considered the VV candidate jet. It is required to have $T_{YWW} > 0.6$, corresponding to an approximately 60 (1)% signal (background) efficiency for jets with $m_Y < 250$ GeV, which is the boundary of the training mass range. The performance of the tagger at this working point is similar for all m_Y beneath this threshold, as shown in Ref. [46]. If the same AK8 jet has both the highest T_{Xbb} and T_{YWW} score in the event, it is classified as the $b\bar{b}$ candidate and the next-highest T_{YWW} scoring jet is considered the VV candidate, where the T_{Xbb} score of the $b\bar{b}$ candidate and the T_{YWW} score of the VV candidate are denoted T^{bb}_{Xbb} and T^{VV}_{YWW}, respectively. The fraction of signal events in which this occurs and that pass our offline selections is found to be less than 1%. All the p_T and tagger selections are jointly optimized for the most stringent expected exclusion limits for a range of m_X and m_Y points.

The search is performed in events passing these selections, referred to as the SP region, binned in the two-dimensional (2D) plane of the VV candidate jet's regressed mass (m^{VV}_{reg}) and the invariant mass of the system composed of the $b\bar{b}$ and VV candidate jets, representing the reconstructed m_Y and m_X (m^{rec}_Y and m^{rec}_X), respectively. The SF region, used to estimate the QCD multijet background, is defined by inverting the tagger selections for both jets. Finally, separate VP and VF regions, defined using the m^{bb}_{reg} sidebands, are used to validate the background estimation technique.

5.2 Semimerged category

The semimerged search targets the $0.1m_X \lesssim m_Y < m_X$ mass range where the hadronic decays of the two V bosons produce two distinct AK8 jets, as opposed to a single jet like in the fully merged category. Therefore, the semimerged category selects events containing at least three AK8 jets—each with $p_T > 200\,\text{GeV}$, $|\eta| < 2.4$, and $m_{reg} > 50\,\text{GeV}$—including an AK8 jet from the $H \to b\bar{b}$ decay and two AK8 jets from the V bosons. The PARTICLENET model is used to target the $H \to b\bar{b}$ jet, as well as the two $V \to q\bar{q}$ jets from the Y decay using a discriminant T_{Wqq} derived from its outputs.

Of the three highest p_T AK8 jets that pass the above selection, the jet with the highest PARTICLENET T_{Xbb} score is considered the $b\bar{b}$ candidate jet, and is required to have $100 < m_{reg} < 150\,\text{GeV}$ ($75 < m_{reg} < 100\,\text{GeV}$ or $150 < m_{reg} < 175\,\text{GeV}$) in the SR (VR). The two remaining AK8 jets are considered $V \to q\bar{q}$ candidates, and must have $70 < m_{reg} < 100\,\text{GeV}$ and pass a loose working point of the T_{Wqq} discriminant yielding a signal efficiency that ranges from 60 to 95% for jet p_T between 200 and 800 GeV.

The SP region of the semimerged category is then defined by requiring that the T_{Xbb} score of the $b\bar{b}$ candidate jet (T^{bb}_{Xbb}) be greater than the HP WP. As in fully merged category, events are binned in the 2D m^{rec}_Y and m^{rec}_X plane, defined as the invariant masses of the systems of the two $V \to q\bar{q}$ candidate jets and of all three AK8 jets, respectively. The SF region is formed by inverting the T^{bb}_{Xbb} score requirement, while the VRs are defined using the m^{bb}_{reg} sidebands. In order to ensure orthogonality of the two categories, events passing the fully merged selections are additionally rejected if they contain two AK8 jets with masses between 60–110 GeV that pass working points of the T_{Wqq} discriminant corresponding to a signal efficiency of 60%.

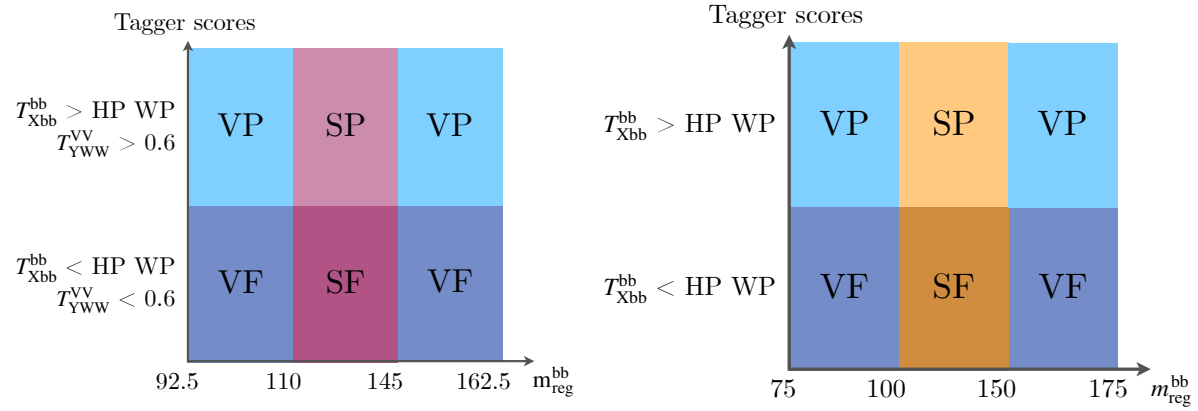

Figure 2: Schematic of the event categorization into the signal pass (SP), signal fail (SF), validation pass (VP), and validation fail (VF) regions for the fully merged (left) and semimerged (right) categories. The pass and fail tagging regions of the fully merged and semimerged categories are determined by application of the high purity (HP) working point (WP) of the T_{Xbb} tagger to the $b\bar{b}$ candidate jet (T^{bb}_{Xbb}). In the fully merged category, the pass and fail tagging regions are additionally defined by application of the T_{YWW} tagger to the $Y \to VV \to 4q$ candidate jet (T^{VV}_{YWW}).

6 Background estimation

The search is performed in the SP regions of the two categories using a 2D binned likelihood model in m^{rec}_X and m^{rec}_Y. The background in these regions is dominated by QCD multijet events,

whose yield is estimated using the product of data in the fail regions and polynomial "transfer functions" [47–49], as described below. Minor backgrounds include t and V backgrounds, which are modeled using the Monte Carlo (MC) simulations described in Section 3. The corresponding systematic and statistical uncertainties are incorporated in the final statistical analysis through nuisance parameters in the likelihood model.

6.1 Fully merged category

In the fully merged category, both the $T^{\mathrm{bb}}_{\mathrm{Xbb}}$ and $T^{\mathrm{VV}}_{\mathrm{YWW}}$ selections are inverted to increase the sample size in the fail region. Although PART has also been trained to be decorrelated with the jet mass, there remains a high likelihood that the $T^{\mathrm{VV}}_{\mathrm{YWW}}$ selection may affect the shape of the $m^{\mathrm{rec}}_{\mathrm{Y}}$, i.e., $m^{\mathrm{VV}}_{\mathrm{reg}}$, observable. To model the expected effect, we first determine a 2D fail-to-pass transfer function from QCD simulation alone, $R^{\mathrm{sim}}(m_{\mathrm{X}}, m_{\mathrm{Y}})$, which is used in conjunction with a second $R^{\mathrm{data}}(m_{\mathrm{X}}, m_{\mathrm{Y}})$ transfer function to correct for any residual differences in data. The product $R(m_{\mathrm{X}}, m_{\mathrm{Y}})$ is the overall fail-to-pass transfer function:

$$R(m_{\mathrm{X}}, m_{\mathrm{Y}}) = R^{\mathrm{sim}}(m_{\mathrm{X}}, m_{\mathrm{Y}})\, R^{\mathrm{data}}(m_{\mathrm{X}}, m_{\mathrm{Y}}), \tag{2}$$

where $R^{\mathrm{sim}}(m_{\mathrm{X}}, m_{\mathrm{Y}})$ and $R^{\mathrm{data}}(m_{\mathrm{X}}, m_{\mathrm{Y}})$ are both chosen to be 2D Bernstein polynomials in m_{X} and m_{Y} [50]:

$$R(m_{\mathrm{X}}, m_{\mathrm{Y}}) = \sum_{k=0}^{n_{m_{\mathrm{X}}}} \sum_{l=0}^{n_{m_{\mathrm{Y}}}} a_{k,l} \left[b_{k,n_{m_{\mathrm{X}}}}(m_{\mathrm{X}})\, b_{l,n_{m_{\mathrm{Y}}}}(m_{\mathrm{Y}}) \right], \tag{3}$$

where $n_{m_{\mathrm{X}}}$ and $n_{m_{\mathrm{Y}}}$ are the orders of the polynomial in m_{X} and m_{Y}, respectively; and $b_{k,n_{m_{\mathrm{X}}}}(m_{\mathrm{X}})$ and $b_{l,n_{m_{\mathrm{Y}}}}(m_{\mathrm{Y}})$ are the kth and l^{th} Bernstein basis functions of order $n_{m_{\mathrm{X}}}$ and $n_{m_{\mathrm{Y}}}$, respectively. The coefficients of the polynomial, $a_{k,l}$, are determined through a simultaneous maximum likelihood fit to the data in the fail and pass regions.

The $R^{\mathrm{sim}}(m_{\mathrm{X}}, m_{\mathrm{Y}})$ function is obtained by a dedicated maximum likelihood fit to QCD simulations in the fail and pass regions, with its order in both $m^{\mathrm{rec}}_{\mathrm{X}}$ and $m^{\mathrm{rec}}_{\mathrm{Y}}$ determined to be 1 by Fisher F-tests [51] for background-only fits to the data in the signal region. The $R^{\mathrm{data}}(m_{\mathrm{X}}, m_{\mathrm{Y}})$ is determined through a fit to data in the signal fail and pass regions using the predetermined $R^{\mathrm{sim}}(m_{\mathrm{X}}, m_{\mathrm{Y}})$; its orders are determined to be 2 and 1 in $m^{\mathrm{rec}}_{\mathrm{X}}$ and $m^{\mathrm{rec}}_{\mathrm{Y}}$, respectively. The measured $R^{\mathrm{sim}}(m_{\mathrm{X}}, m_{\mathrm{Y}})$ and total $R(m_{\mathrm{X}}, m_{\mathrm{Y}})$ transfer functions, as measured in the signal region, are shown in Fig. 3, with the same binning in $(m_{\mathrm{X}}, m_{\mathrm{Y}})$ as used in the maximum likelihood fit to data. To achieve an adequate sample size in each bin, the bin widths along the m_{X} axis are gradually increased at higher masses.

6.2 Semimerged category

To estimate the QCD multijet background in the pass regions, the data in the respective fail regions are used as independent control regions to model its shape. In the semimerged category, the SF region is defined by inverting the $T^{\mathrm{bb}}_{\mathrm{Xbb}}$ selection alone such that the shape of the multijet background regions is obtained directly from the shape in the fail region.

Explicitly, the QCD multijet yield in the ith $m^{\mathrm{rec}}_{\mathrm{X}}$ and j^{th} $m^{\mathrm{rec}}_{\mathrm{Y}}$ bin in the fail regions (binned identically to the pass region) is represented by a floating parameter in the likelihood, $N^{ij}_{\mathrm{QCD\ fail}}$. The initial value of $N^{ij}_{\mathrm{QCD\ fail}}$ is set as the difference between the data and the total simulated backgrounds in that bin. The QCD yield estimate in the corresponding bin of the pass region,

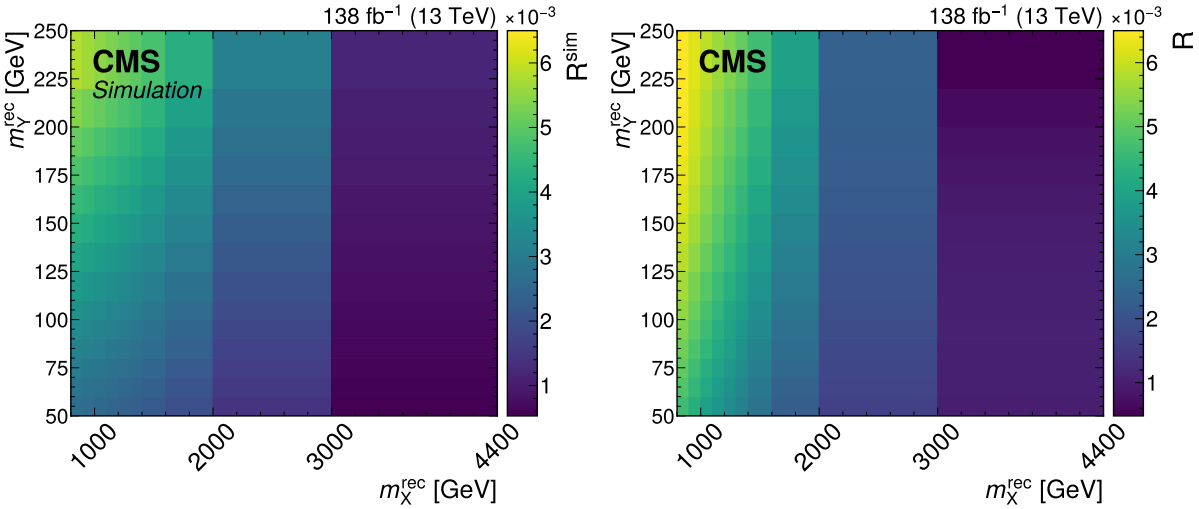

Figure 3: Measured transfer functions $R^{\text{sim}}(m_X, m_Y)$ (left) and $R(m_X, m_Y)$ (right) between the signal pass (SP) and signal fail (SF) regions of the fully merged category used to estimate the QCD multijet background contribution.

$N^{ij}_{\text{QCD pass}}$, is then determined by the product of $N^{ij}_{\text{QCD fail}}$ and a 2D pass-to-fail transfer function, $R(m_X, m_Y)$, evaluated at that bin:

$$N^{ij}_{\text{QCD pass}} = R(m^i_X, m^j_Y)\, N^{ij}_{\text{QCD fail}}. \tag{4}$$

The function R serves to model any potential differences in the shape of the multijet background in the fail and pass regions, with its form chosen to be a 2D Bernstein polynomial in m_X and m_Y as in Eq. 3. Its order in both m_X^{rec} and m_Y^{rec} is determined by Fisher F-tests to be 0, i.e., a constant R. This indicates that the shapes of the QCD multijet background in both regions are indeed consistent, which is not unexpected since the ParticleNet tagger has been shown to be successfully decorrelated with the jet mass [43]. The fitted value is $R(m_X, m_Y) = 0.024 \pm 0.002$.

6.3 Validation

This background estimation procedure is first validated for both categories in dedicated, background-dominated VRs, defined in Section 5 and shown in Figs. 4 and 5. The lower panels show the pull per bin, defined as the difference between the data and predicted event yields divided by the statistical uncertainty associated with the data assuming a Poisson distribution, σ_{stat}. Also shown in the lower panels is a gray band indicating the systematic uncertainty in the pulls, estimated by dividing the corresponding systematic uncertainty in the main panel by σ_{stat}. The agreement between the data and background model in the VRs is quantified via two-sample goodness of fit tests using the saturated model test statistic [52]. This yields p-values [53] of 0.85 and 0.11 for the semimerged and fully merged categories, respectively, indicating no significant discrepancies. The goodness of fit tests are then repeated for the data and the background models in the SRs, yielding p-values of 0.76 and 0.27, respectively. In both categories, bias tests were performed in pseudodata by injecting various signal mass hypotheses at cross sections corresponding to their respective expected limits. The injected signal cross sections were successfully recovered in all such tests, indicating no significant bias in the signal extraction process.

To avoid biasing the analysis, genuine data in the SR pass regions are not observed during their optimization. Instead, the expected R functions are derived through fits to the data in

the VRs, and are then used in conjunction with the data in the SF regions to estimate the SP region background yields. The VRs are used only to finalize the selections and validate the background estimation strategy. They are not used in the search and do not affect the results presented in this paper.

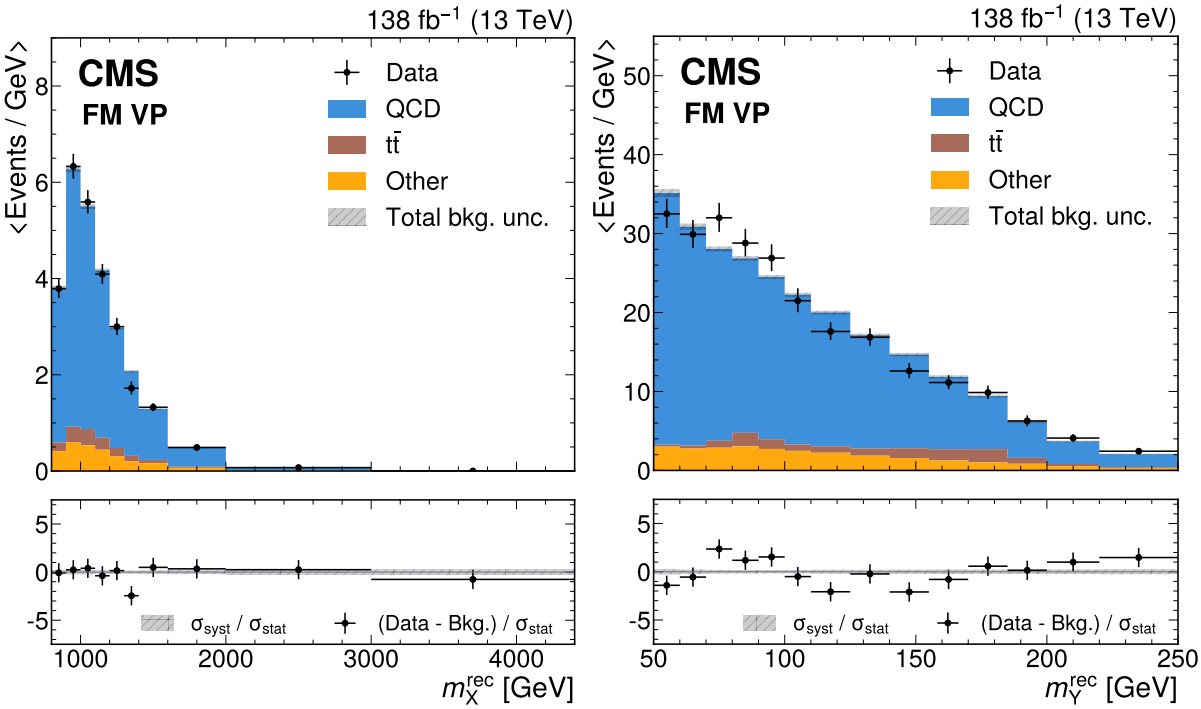

Figure 4: Projected distributions of the m_X^{rec} (left) and m_Y^{rec} (right) observables in the validation pass (VP) region of the fully merged (FM) category, after a background-only maximum likelihood fit to the data. The upper panels show the data and fitted background estimates, as well as the ± 1 standard deviation uncertainty in the total background estimate (σ_{syst}) per bin, divided by the respective bin widths, in gray. The vertical error bars for the data represent the statistical uncertainty, while the horizontal bars represent the bin widths. The lower panels show the pull per bin, defined as $(\text{data} - \text{Bkg.})/\sigma_{stat}$, as well as a gray band indicating the systematic uncertainty in the pulls, estimated by dividing the corresponding systematic uncertainty in the main panel by σ_{stat}.

7 Systematic uncertainties

Several sources of systematic uncertainties in the signal and background estimation are considered and summarized in Table 1. The dominant source of uncertainty for both the fully merged and semimerged categories is the statistical uncertainty in the QCD multijet background estimate. The impact of a nuisance parameter on a parameter of interest is defined as the shift in the parameter of interest when the nuisance parameter is shifted from its best-fit value by its uncertainty, while profiling all other parameters [54]. The largest relative impact for a single transfer factor parameter, defined as the ratio of its impact on the best-fit signal strength to the total post-fit uncertainty in the signal strength, is 46% and 28% for the fully merged and semimerged categories, respectively, evaluated for the signal mass points with the largest global significances in each category.

In the fully merged category, this is followed by uncertainties in the signal efficiencies of the ParticleNet T_{Xbb} and ParT T_{YWW} selections, with relative impacts of 17 and 20%, respec-

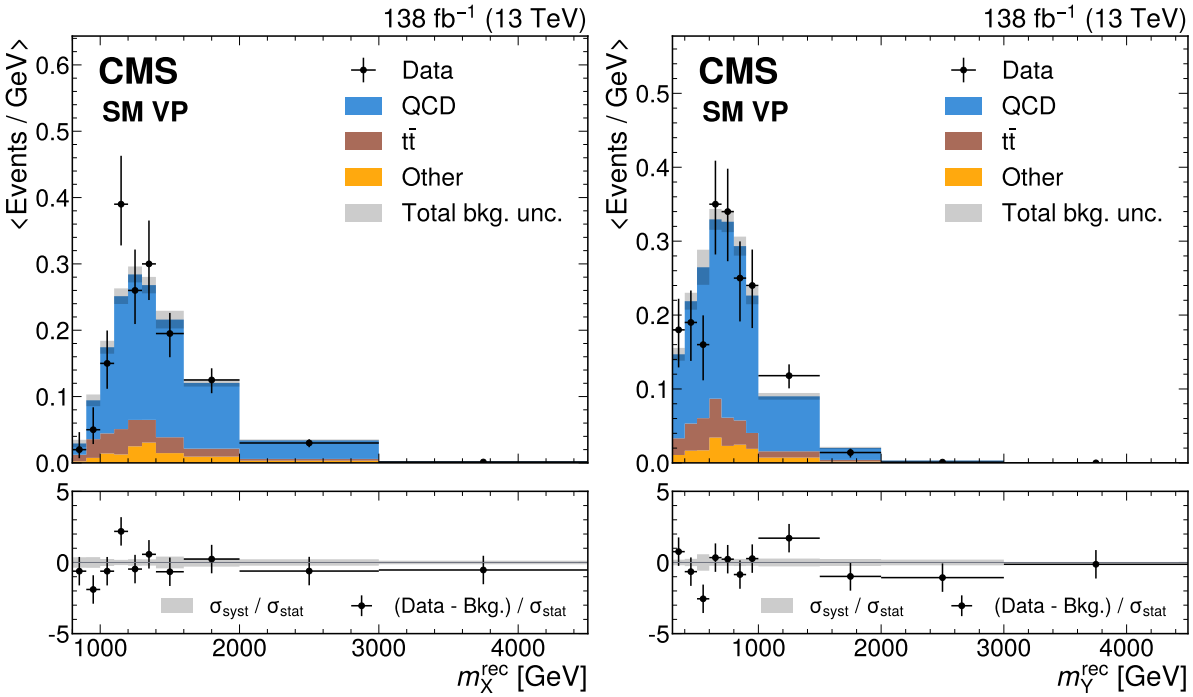

Figure 5: Projected distributions of the m_X^{rec} (left) and m_Y^{rec} (right) observables in the validation pass (VP) region of the semimerged (SM) category, after a background-only maximum likelihood fit to the data. The upper panels show the data and fitted background estimates, as well as the ± 1 standard deviation uncertainty in the total background estimate (σ_{syst}) per bin, divided by the respective bin widths, in gray. The vertical error bars for the data represent the statistical uncertainty, while the horizontal bars represent the bin widths. The lower panels show the pull per bin, defined as $(\text{data} - \text{Bkg.})/\sigma_{stat}$, as well as a gray band indicating the systematic uncertainty in the pulls, estimated by dividing the corresponding systematic uncertainty in the main panel by σ_{stat}.

tively. The T_{Xbb} selection efficiency scale factors are measured by comparing data and simulation in a data sample dominated by $\mathrm{g} \to \mathrm{b\bar{b}}$ jets, obtained using the "sfBDT" method [41], which uses a boosted decision tree to select $\mathrm{g} \to \mathrm{b\bar{b}}$ jets that are similar to the resonant $\mathrm{H} \to \mathrm{b\bar{b}}$ signal. The resulting scale factors range from 0.9 to 1.2 for the HP WP with uncertainties ranging from 4 to 10%, depending on the jet p_{T} and data-taking era. The dominant uncertainties in the scale factor include the effects of applying different assumptions for reweighting simulation to data as well as statistical uncertainties. The T_{YWW} selection efficiency scale factors are evaluated using a new technique based on the ratio of the primary Lund jet plane [46, 55, 56] densities of each individual subjet between data and simulation. The scale factors for the latter range from 0.9 to 1.2 with uncertainties of $\approx$10% for highly boosted jets, i.e., from signals with a high $m_{\mathrm{X}}/m_{\mathrm{Y}}$ ratio, and range from 20 to 50% for less boosted jets. The dominant uncertainties in this method include an uncertainty stemming from corrections to simulations used to measure the Lund jet plane densities, as well as an uncertainty in the quark-to-subjet association.

In the semimerged category, the uncertainties in the T_{Xbb} and T_{Wqq} tagging efficiency have impacts of 13 and 9%, respectively. The same T_{Xbb} selection efficiency scale factors are applied, while for the T_{Wqq} selection, the efficiency is calibrated by comparing the efficiencies in data and simulation in a lepton plus jets data sample dominated by $\mathrm{t\bar{t}}$ events. The scale factors for the T_{Wqq} tagger WP used in the semimerged category range from 0.8 to 0.9 with uncertainties in the 5–10% range depending on the jet p_{T}.

Other significant sources of experimental uncertainty include the scale and resolution of the regressed jet mass and reconstructed jet energy [57] in data versus simulation. Jet mass corrections and uncertainties are measured in a data sample enriched in $\mathrm{t\bar{t}}$ events, using AK8 jets originating from hadronic W boson decays [58], with impacts of 26 and 6% in the fully merged and semimerged categories, respectively. Jet energy corrections and uncertainties constitute 2 and 3%, respectively, for the two categories. Finally, there are large statistical uncertainties related to the MC simulations of the signal and less important t and V backgrounds, reaching 30% in some bins of the SRs.

Less important sources of uncertainty include those related to the renormalization and factorization scales, PDFs, Higgs boson branching fractions, integrated luminosity [13, 14], pileup effects, and trigger efficiencies, all of which have sub-percent-level impacts.

8 Results

For both search categories, a 2D binned maximum likelihood fit is performed to the observed $m_{\mathrm{X}}^{\mathrm{rec}}$ and $m_{\mathrm{Y}}^{\mathrm{rec}}$ distributions, simultaneously in the fail and pass regions, for a wide range of potential X and Y mass points. The m_{X} and m_{Y} points are separated per category based on which one yields a lower expected exclusion limit; hence, the two categories themselves are not fit simultaneously. The following results have been determined using the CMS statistical analysis tool COMBINE [54], based on the ROOFIT [59] and ROOSTATS [60] frameworks.

The data and fitted estimates for backgrounds and the signal hypotheses with the largest statistical significances for the fully merged and semimerged categories are shown in Figs. 6 and 7, respectively, projected onto the $m_{\mathrm{X}}^{\mathrm{rec}}$ and $m_{\mathrm{Y}}^{\mathrm{rec}}$ observables. Figure 8 shows the 2D pull plots for both categories. The largest deviation from the background-only hypothesis is observed in the fully merged category for $m_{\mathrm{X}} = 900\,\mathrm{GeV}$ and $m_{\mathrm{Y}} = 80\,\mathrm{GeV}$ with a local (global) significance of 3.3 (below 1.0) standard deviations. In the semimerged category, the largest deviation is observed for $m_{\mathrm{X}} = 1200\,\mathrm{GeV}$ and $m_{\mathrm{Y}} = 900\,\mathrm{GeV}$ with a local (global) significance of 1.7 (below 1.0) standard deviations.

Table 1: Sources of systematic uncertainties and the range of variations in the yields of the specified processes in the fully merged (FM) and semimerged (SM) categories.

Source	Processes affected	Uncertainty (FM)	Uncertainty (SM)
T_{YWW} signal efficiency	Signal	6–50%	—
T_{Xbb} signal efficiency	Signal	4–10%	
T_{Wqq} signal efficiency	Signal	—	9%
$H \to b\bar{b}$ branching fraction	Signal, $H \to b\bar{b}$	1.25%	
R function parameters	QCD multijet	8–20%	6%
Parton showering	All simulations	1–9%	
Jet energy scale and resolution	All simulations	1–3%	
Jet mass scale and resolution	All simulations	1–4%	
MC statistical uncertainty	Signal	1–10%	
MC statistical uncertainty	$t\bar{t}$	1–30%	
Renorm. and fact. scales	All simulations	7–10%	
PDF	All simulations	1%	
Integrated luminosity	All simulations	2%	
Pileup	All simulations	1%	
Trigger efficiencies	All simulations	<1%	1–2%

Expected and observed exclusion limits at 95% confidence level (CL) are derived on the $X \to HY$ production cross section assuming a 100% branching fraction for the $Y \to WW$ decays and standard model branching fractions for the subsequent $VV \to 4q$ decays. They are shown in the 2D m_X vs. m_Y plane in Fig. 9 as well as in one dimension for different m_X points in Fig. 10. The results can be interpreted in the context of $Y \to ZZ$ decays by dividing the upper limits by a factor of 0.73 (0.78) in the fully merged (semimerged) category, to account for the lower selection efficiency of $Y \to ZZ$ with respect to $Y \to WW$, as explained in Section 5. The separation between the fully merged and semimerged categories is governed by the fraction of signal $Y \to VV$ jets containing four quarks and is depicted by a dashed line in Fig. 9 and a separation between sets of points in Fig. 10. The loss of sensitivity at higher m_Y in Fig. 10 corresponds to points where the decay products of the Higgs boson are no longer captured entirely within an AK8 jet and is similarly reflected by the increase in the limits along the boundary denoting kinematically allowed masses in Fig. 9.

The limits are calculated using asymptotic approximations for the profile likelihood ratio test statistic [53, 61] and the CL_s [62, 63] criterion. The validity of the asymptotic approximation was tested for a subset of signals whose distributions lie predominantly in bins with less than ten expected events. For all such signals, the limits calculated using the asymptotic approximation agreed within 15% with those calculated using the distribution of test statistics obtained from pseudodata, motivating the use of the asymptotic approximation for the full range of signal mass points.

The results were further interpreted in the context of asymmetric cascade decays in a two-real-scalar-singlet model [4], which introduces two real singlet fields S and X to the standard model Higgs sector. Scans of the vacuum expectation values of these new scalars, v_S and v_X, and the mixing angles between the Higgs field and the new fields as well as among themselves, θ_{HS}, θ_{HX}, and θ_{SX}, are performed to obtain the maximally allowed product of cross section and branching fraction to $b\bar{b}VV$ for all mass points under consideration. These scans employ the narrow width approximation to factorize production cross sections and branching fractions, consistent with the signal samples used in this analysis. No mass exclusions can be made for any masses of the X and Y bosons under this model, although for $m_X < 1.4$ and $m_Y < 0.6\,\text{TeV}$,

the observed limits are about a factor of 10 higher than the maximum prediction of this model.

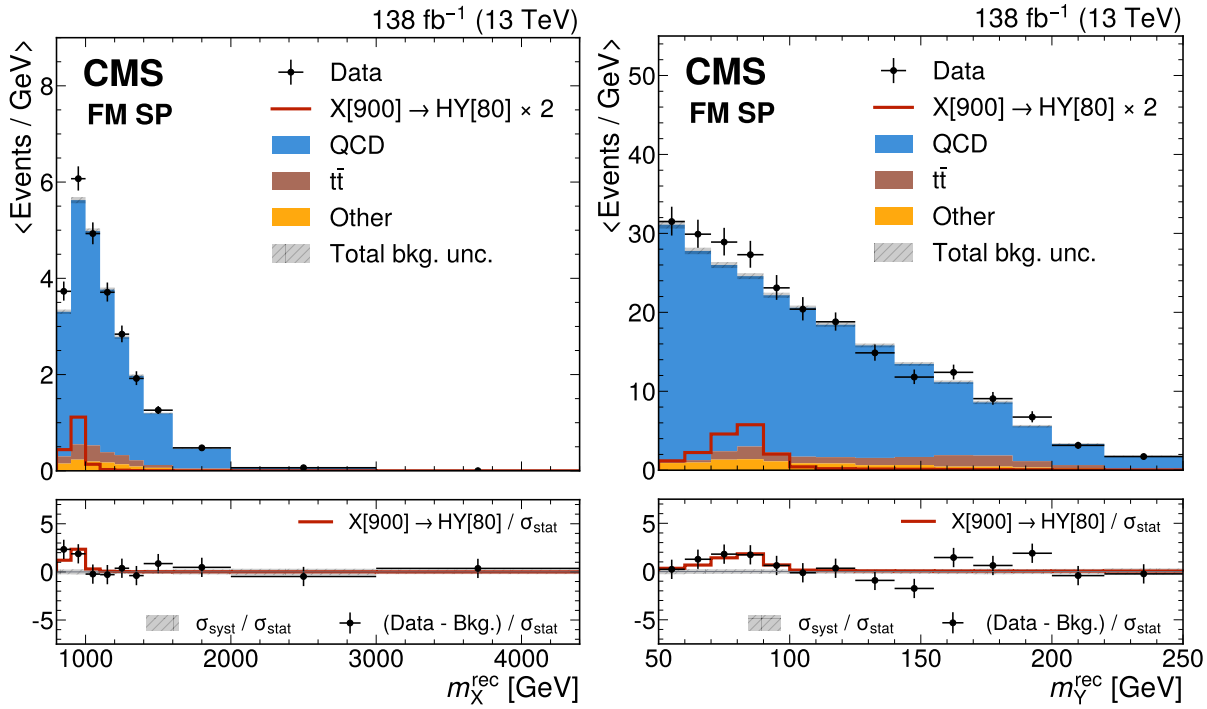

Figure 6: Projected distributions of the m_X^{rec} (left) and m_Y^{rec} (right) observables in the signal pass (SP) region of the fully merged (FM) category, after a maximum likelihood fit to the data with an $X \to HY \to b\bar{b}WW$ signal with $m_X = 900\,\text{GeV}$ and $m_Y = 80\,\text{GeV}$ and product of best-fit production cross section and branching fraction of 15 fb. The signal distribution has been scaled by a factor of two in the upper panels to help distinguish it from the background distributions. The lower panels show the pull per bin, defined as $(\text{data} - \text{Bkg.})/\sigma_{\text{stat}}$, as well as a gray band indicating the systematic uncertainty in the pulls, estimated by dividing the corresponding systematic uncertainty in the main panel by σ_{stat}.

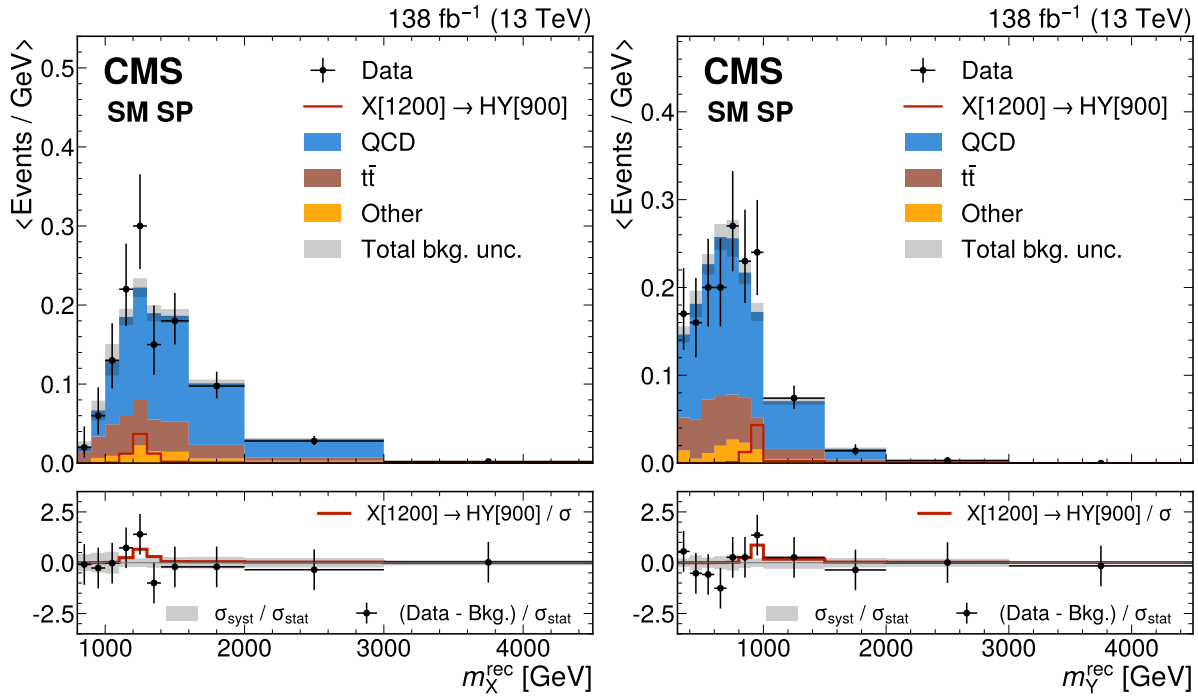

Figure 7: Projected distributions of the m_X^{rec} (left) and m_Y^{rec} (right) observables in the signal pass (SP) region of the semimerged (SM) category, after a maximum likelihood fit to the data with an $X \to HY \to b\bar{b}WW$ signal with $m_X = 1200\,GeV$ and $m_Y = 900\,GeV$ and product of best-fit production cross section and branching fraction of 250 fb. The lower panels show the pull per bin, defined as $(data - Bkg.)/\sigma_{stat}$, as well as a gray band indicating the systematic uncertainty in the pulls, estimated by dividing the corresponding systematic uncertainty in the main panel by σ_{stat}.

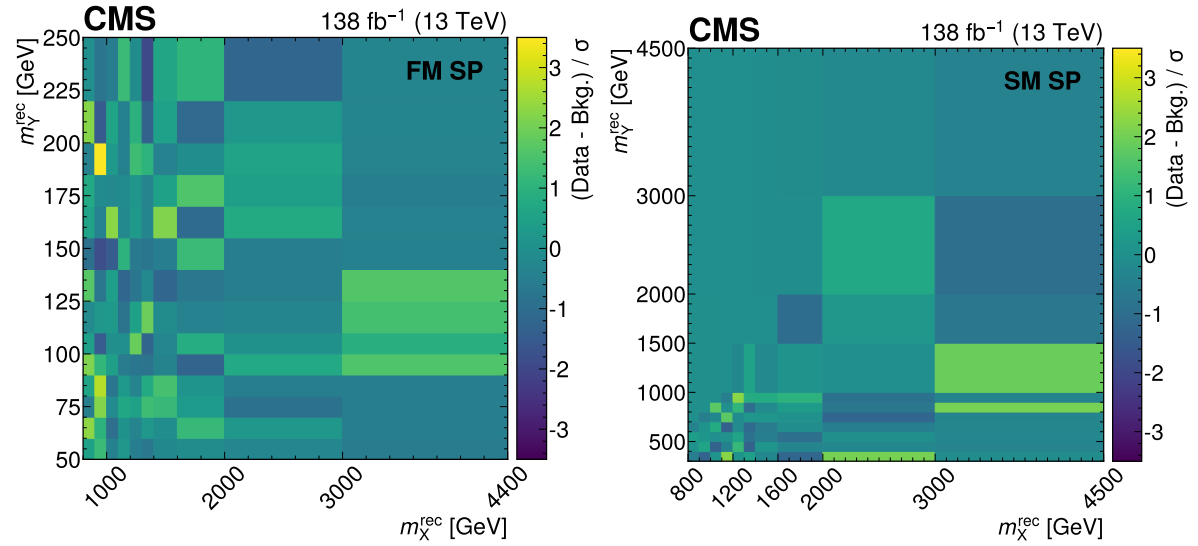

Figure 8: The 2D pulls in the m_X^{rec} and m_Y^{rec} observables in the signal pass (SP) regions of the fully merged (FM, left) and semimerged (SM, right) categories, after a maximum likelihood fit to the data with an $X \to HY \to b\bar{b}WW$ signal with $m_X = 900\,GeV$ and $m_Y = 80\,GeV$, and $m_X = 1200\,GeV$ and $m_Y = 900\,GeV$, respectively. Pulls are defined as $(data - Bkg.)/\sigma$, where σ is the sum in quadrature of the background uncertainty and the statistical uncertainty associated with the data assuming a Poisson distribution.

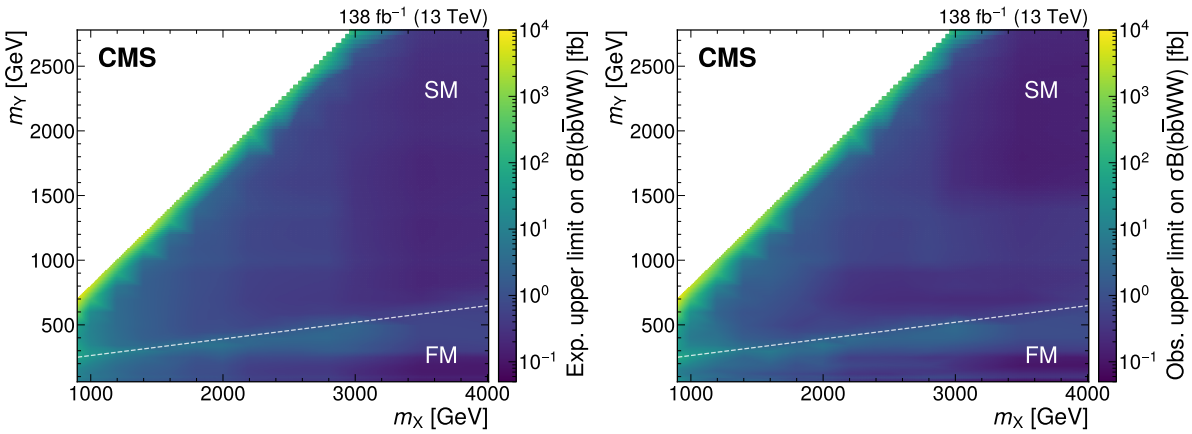

Figure 9: Median expected (left) and observed (right) upper limits at 95% CL on the product of production cross section and branching fraction for $X \to HY \to b\bar{b}WW$ on the 2D m_X and m_Y plane. The dashed line separates the mass points considered in the fully merged (FM) and semimerged (SM) categories.

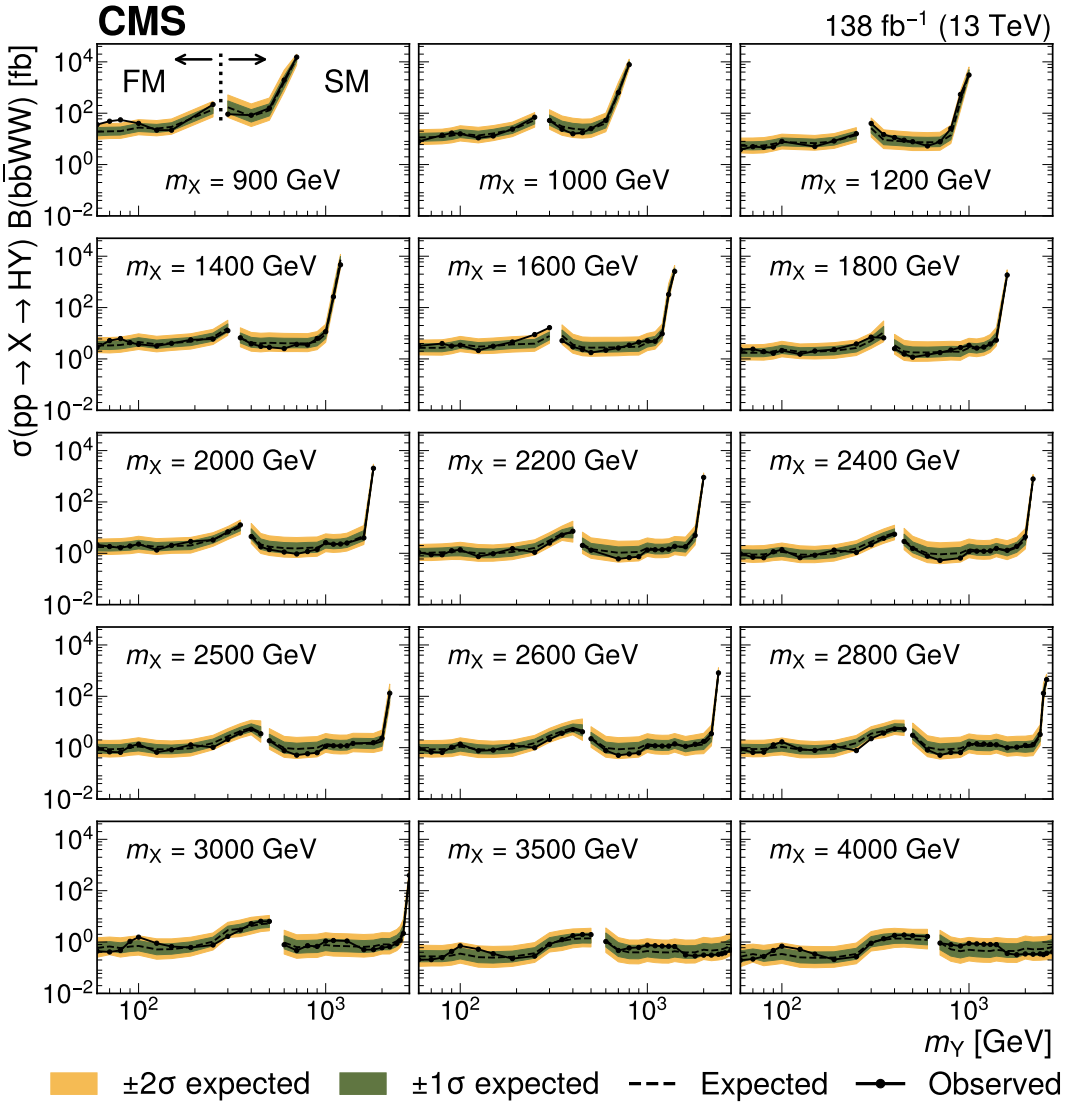

Figure 10: Expected and observed upper limits at 95% CL on the product of production cross section and branching fraction for $X \to HY \to b\bar{b}WW$ signals. The dashed and solid black lines represent median expected and observed limits, respectively. The inner (green) and outer (yellow) bands represent the ± 1 and ± 2 standard deviations for the expected limits, respectively. The left and right set of points in each panel correspond to those considered in the fully merged (FM) and semimerged (SM) categories, respectively.

9 Summary

A search has been performed for a heavy scalar resonance X decaying to a Higgs boson (H) and Higgs-like scalar boson (Y) in the two bottom quark ($H \to b\bar{b}$) and four quark ($Y \to VV \to 4q$) final state, where V denotes a W or Z boson. The search targets Lorentz-boosted $X \to HY$ production where the daughter quarks from the Higgs and Y bosons are merged within large-area jets. A mass-decorrelated graph neural network tagger, known as PARTICLENET, was used to select $H \to b\bar{b}$ and $V \to q\bar{q}$ jets while the new "particle transformer" is used for fully merged $Y \to VV$ jets. The signal is extracted from a two-dimensional maximum likelihood fit to data binned in the reconstructed Y and X masses. The dominant quantum chromodynamics multijet background is estimated using control regions in data with the tagger score selections inverted. Other minor backgrounds including top quark and V plus jets are estimated using Monte Carlo simulations. No significant excess is observed in the data above the standard model background expectation. Upper limits at 95% confidence level as low as 0.2 fb are set for the product of resonant $X \to HY \to b\bar{b}VV$ production cross section and branching fraction for various X and Y masses. This is the first search for scalar resonances in the all-hadronic $b\bar{b}VV$ final state at the LHC.

Acknowledgments

We congratulate our colleagues in the CERN accelerator departments for the excellent performance of the LHC and thank the technical and administrative staffs at CERN and at other CMS institutes for their contributions to the success of the CMS effort. In addition, we gratefully acknowledge the computing centers and personnel of the Worldwide LHC Computing Grid and other centers for delivering so effectively the computing infrastructure essential to our analyses. Finally, we acknowledge the enduring support for the construction and operation of the LHC, the CMS detector, and the supporting computing infrastructure provided by the following funding agencies: SC (Armenia), BMBWF and FWF (Austria); FNRS and FWO (Belgium); CNPq, CAPES, FAPERJ, FAPERGS, and FAPESP (Brazil); MES and BNSF (Bulgaria); CERN; CAS, MoST, and NSFC (China); MINCIENCIAS (Colombia); MSES and CSF (Croatia); RIF (Cyprus); SENESCYT (Ecuador); ERC PRG, TARISTU24-TK10 and MoER TK202 (Estonia); Academy of Finland, MEC, and HIP (Finland); CEA and CNRS/IN2P3 (France); SRNSF (Georgia); BMFTR, DFG, and HGF (Germany); GSRI (Greece); NKFIH (Hungary); DAE and DST (India); IPM (Iran); SFI (Ireland); INFN (Italy); MSIT and NRF (Republic of Korea); MES (Latvia); LMTLT (Lithuania); MOE and UM (Malaysia); BUAP, CINVESTAV, CONACYT, LNS, SEP, and UASLP-FAI (Mexico); MOS (Montenegro); MBIE (New Zealand); PAEC (Pakistan); MES, NSC, and NAWA (Poland); FCT (Portugal); MESTD (Serbia); MICIU/AEI and PCTI (Spain); MOSTR (Sri Lanka); Swiss Funding Agencies (Switzerland); MST (Taipei); MHESI (Thailand); TUBITAK and TENMAK (Türkiye); NASU (Ukraine); STFC (United Kingdom); DOE and NSF (USA).

Individuals have received support from the Marie-Curie program and the European Research Council and Horizon 2020 Grant, contract Nos. 675440, 724704, 752730, 758316, 765710, 824093, 101115353, 101002207, 101001205, and COST Action CA16108 (European Union); the Leventis Foundation; the Alfred P. Sloan Foundation; the Alexander von Humboldt Foundation; the Science Committee, project no. 22rl-037 (Armenia); the Fonds pour la Formation à la Recherche dans l'Industrie et dans l'Agriculture (FRIA) and Fonds voor Wetenschappelijk Onderzoek contract No. 1228724N (Belgium); the Beijing Municipal Science & Technology Commission, No. Z191100007219010, the Fundamental Research Funds for the Central Universities, the Ministry of Science and Technology of China under Grant No. 2023YFA1605804, the Natural Science

Foundation of China under Grant No. 12535004, and USTC Research Funds of the Double First-Class Initiative No. YD2030002017 (China); the Ministry of Education, Youth and Sports (MEYS) of the Czech Republic; the Shota Rustaveli National Science Foundation, grant FR-22-985 (Georgia); the Deutsche Forschungsgemeinschaft (DFG), among others, under Germany's Excellence Strategy – EXC 2121 "Quantum Universe" – 390833306, and under project number 400140256 - GRK2497; the Hellenic Foundation for Research and Innovation (HFRI), Project Number 2288 (Greece); the Hungarian Academy of Sciences, the New National Excellence Program - ÚNKP, the NKFIH research grants K 131991, K 133046, K 138136, K 143460, K 143477, K 146913, K 146914, K 147048, 2020-2.2.1-ED-2021-00181, TKP2021-NKTA-64, and 2025-1.1.5-NEMZ_KI-2025-00004 (Hungary); the Council of Science and Industrial Research, India; ICSC – National Research Center for High Performance Computing, Big Data and Quantum Computing, FAIR – Future Artificial Intelligence Research, and CUP I53D23001070006 (Mission 4 Component 1), funded by the NextGenerationEU program (Italy); the Latvian Council of Science; the Ministry of Education and Science, project no. 2022/WK/14, and the National Science Center, contracts Opus 2021/41/B/ST2/01369, 2021/43/B/ST2/01552, 2023/49/B/ST2/03273, and the NAWA contract BPN/PPO/2021/1/00011 (Poland); the Fundação para a Ciência e a Tecnologia, grant CEECIND/01334/2018 (Portugal); the National Priorities Research Program by Qatar National Research Fund; MICIU/AEI/10.13039/501100011033, ERDF/EU, "European Union NextGenerationEU/PRTR", and Programa Severo Ochoa del Principado de Asturias (Spain); the Chulalongkorn Academic into Its 2nd Century Project Advancement Project, the National Science, Research and Innovation Fund program IND_FF_68_369_2300_097, and the Program Management Unit for Human Resources & Institutional Development, Research and Innovation, grant B39G680009 (Thailand); the Kavli Foundation; the Nvidia Corporation; the SuperMicro Corporation; the Welch Foundation, contract C-1845; and the Weston Havens Foundation (USA).

Data availability

Release and preservation of data used by the CMS Collaboration as the basis for publications is guided by the CMS data preservation, re-use and open access policy.

References

[1] G. C. Branco et al., "Theory and phenomenology of two-Higgs-doublet models", *Phys. Rept.* **516** (2012) 1, doi:10.1016/j.physrep.2012.02.002, arXiv:1106.0034.

[2] N. Craig, J. Galloway, and S. Thomas, "Searching for signs of the second Higgs doublet", 2013. arXiv:1305.2424.

[3] F. Domingo and S. Paßehr, "About the bosonic decays of heavy Higgs states in the (N)MSSM", *Eur. Phys. J. C* **82** (2022) 962, doi:10.1140/epjc/s10052-022-10919-4, arXiv:2207.05776.

[4] T. Robens, T. Stefaniak, and J. Wittbrodt, "Two-real-scalar-singlet extension of the SM: LHC phenomenology and benchmark scenarios", *Eur. Phys. J. C* **80** (2020) 151, doi:10.1140/epjc/s10052-020-7655-x, arXiv:1908.08554.

[5] LHC Higgs Cross Section Working Group Collaboration, "Handbook of LHC Higgs Cross Sections: 4. Deciphering the Nature of the Higgs Sector", *CERN Yellow Rep. Monogr.* **2** (2017) 1, doi:10.23731/CYRM-2017-002, arXiv:1610.07922.

[6] CMS Collaboration, "Search for a massive scalar resonance decaying to a light scalar and a Higgs boson in the four b quarks final state with boosted topology", *Phys. Lett. B* **842** (2023) 137392, doi:10.1016/j.physletb.2022.137392, arXiv:2204.12413.

[7] CMS Collaboration, "Search for a new resonance decaying into two spin-0 bosons in a final state with two photons and two bottom quarks in proton-proton collisions at $\sqrt{s}$ = 13 TeV", *JHEP* **05** (2024) 316, doi:10.1007/JHEP05(2024)316, arXiv:2310.01643.

[8] CMS Collaboration, "Search for a heavy Higgs boson decaying into two lighter Higgs bosons in the $\tau\tau$bb final state at 13 TeV", *JHEP* **11** (2021) 057, doi:10.1007/JHEP11(2021)057, arXiv:2106.10361.

[9] ATLAS Collaboration, "Search for a resonance decaying into a scalar particle and a Higgs boson in the final state with two bottom quarks and two photons with 199 fb^{-1} of data collected at $\sqrt{s} = 13$ TeV and $\sqrt{s} = 13.6$ TeV with the ATLAS detector", 2025. arXiv:2510.02857. Submitted to *Phys. Lett. B*.

[10] ATLAS Collaboration, "Search for a resonance decaying into a scalar particle and a Higgs boson in final states with leptons and two photons in proton-proton collisions at $\sqrt{s} = 13$ TeV with the ATLAS detector", *JHEP* **10** (2024) 104, doi:10.1007/JHEP10(2024)104, arXiv:2405.20926.

[11] ATLAS Collaboration, "Search for a new heavy scalar particle decaying into a Higgs boson and a new scalar singlet in final states with one or two light leptons and a pair of τ-leptons with the ATLAS detector", *JHEP* **10** (2023) 009, doi:10.1007/JHEP10(2023)009, arXiv:2307.11120.

[12] CMS Collaboration, "Search for Higgs boson pair production in the $\mathrm{b\bar{b}W^+W^-}$ decay mode in proton-proton collisions at $\sqrt{s}$ = 13 TeV", *JHEP* **07** (2024) 293, doi:10.1007/JHEP07(2024)293, arXiv:2403.09430.

[13] CMS Collaboration, "Precision luminosity measurement in proton-proton collisions at $\sqrt{s} = 13$ TeV in 2015 and 2016 at CMS", *Eur. Phys. J. C* **81** (2021) 800, doi:10.1140/epjc/s10052-021-09538-2, arXiv:2104.01927.

[14] CMS Collaboration, "Precision luminosity measurement in proton-proton collisions at $\sqrt{s} = 13$ TeV with the CMS detector", CMS Physics Analysis Summary CMS-PAS-LUM-20-001, 2025.

[15] HEPData record for this analysis, 2026. doi:10.17182/hepdata.167732.

[16] CMS Collaboration, "The CMS experiment at the CERN LHC", *JINST* **3** (2008) S08004, doi:10.1088/1748-0221/3/08/S08004.

[17] CMS Collaboration, "Development of the CMS detector for the CERN LHC Run 3", *JINST* **19** (2024) P05064, doi:10.1088/1748-0221/19/05/P05064, arXiv:2309.05466.

[18] CMS Collaboration, "Performance of the CMS Level-1 trigger in proton-proton collisions at $\sqrt{s} = 13$ TeV", *JINST* **15** (2020) P10017, doi:10.1088/1748-0221/15/10/P10017, arXiv:2006.10165.

[19] CMS Collaboration, "The CMS trigger system", *JINST* **12** (2017) P01020, doi:10.1088/1748-0221/12/01/P01020, arXiv:1609.02366.

[20] CMS Collaboration, "Performance of the CMS high-level trigger during LHC Run 2", *JINST* **19** (2024) P11021, doi:10.1088/1748-0221/19/11/P11021, arXiv:2410.17038.

[21] J. Alwall et al., "The automated computation of tree-level and next-to-leading order differential cross sections, and their matching to parton shower simulations", *JHEP* **07** (2014) 079, doi:10.1007/JHEP07(2014)079, arXiv:1405.0301.

[22] T. Sjöstrand et al., "An introduction to PYTHIA 8.2", *Comput. Phys. Commun.* **191** (2015) 159, doi:10.1016/j.cpc.2015.01.024, arXiv:1410.3012.

[23] CMS Collaboration, "Extraction and validation of a new set of CMS PYTHIA 8 tunes from underlying-event measurements", *Eur. Phys. J. C* **80** (2020) 4, doi:10.1140/epjc/s10052-019-7499-4, arXiv:1903.12179.

[24] P. Nason, "A new method for combining NLO QCD with shower Monte Carlo algorithms", *JHEP* **11** (2004) 040, doi:10.1088/1126-6708/2004/11/040, arXiv:hep-ph/0409146.

[25] S. Frixione, P. Nason, and G. Ridolfi, "A positive-weight next-to-leading-order Monte Carlo for heavy flavour hadroproduction", *JHEP* **09** (2007) 126, doi:10.1088/1126-6708/2007/09/126, arXiv:0707.3088.

[26] S. Frixione, P. Nason, and C. Oleari, "Matching NLO QCD computations with parton shower simulations: the POWHEG method", *JHEP* **11** (2007) 070, doi:10.1088/1126-6708/2007/11/070, arXiv:0709.2092.

[27] S. Alioli, P. Nason, C. Oleari, and E. Re, "A general framework for implementing NLO calculations in shower Monte Carlo programs: the POWHEG box", *JHEP* **06** (2010) 043, doi:10.1007/JHEP06(2010)043, arXiv:1002.2581.

[28] T. Ježo et al., "An NLO+PS generator for $t\bar{t}$ and Wt production and decay including non-resonant and interference effects", *Eur. Phys. J. C* **76** (2016) 691, doi:10.1140/epjc/s10052-016-4538-2, arXiv:1607.04538.

[29] NNPDF Collaboration, "Parton distributions for the LHC Run II", *JHEP* **04** (2015) 040, doi:10.1007/JHEP04(2015)040, arXiv:1410.8849.

[30] NNPDF Collaboration, "Parton distributions from high-precision collider data", *Eur. Phys. J. C* **77** (2017) 663, doi:10.1140/epjc/s10052-017-5199-5, arXiv:1706.00428.

[31] GEANT4 Collaboration, "GEANT4 – a simulation toolkit", *Nucl. Instrum. Meth. A* **506** (2003) 250, doi:10.1016/S0168-9002(03)01368-8.

[32] CMS Collaboration, "Particle-flow reconstruction and global event description with the CMS detector", *JINST* **12** (2017) P10003, doi:10.1088/1748-0221/12/10/P10003, arXiv:1706.04965.

[33] CMS Collaboration, "Technical proposal for the Phase-II upgrade of the Compact Muon Solenoid", CMS Technical Proposal CERN-LHCC-2015-010, CMS-TDR-15-02, 2015.

[34] M. Cacciari, G. P. Salam, and G. Soyez, "The anti-k_T jet clustering algorithm", *JHEP* **04** (2008) 063, doi:10.1088/1126-6708/2008/04/063, arXiv:0802.1189.

[35] M. Cacciari, G. P. Salam, and G. Soyez, "FastJet user manual", *Eur. Phys. J. C* **72** (2012) 1896, doi:10.1140/epjc/s10052-012-1896-2, arXiv:1111.6097.

[36] CMS Collaboration, "Jet energy scale and resolution in the CMS experiment in pp collisions at 8 TeV", *JINST* **12** (2017) P02014, doi:10.1088/1748-0221/12/02/P02014, arXiv:1607.03663.

[37] D. Bertolini, P. Harris, M. Low, and N. Tran, "Pileup per particle identification", *JHEP* **10** (2014) 059, doi:10.1007/JHEP10(2014)059, arXiv:1407.6013.

[38] CMS Collaboration, "Pileup mitigation at CMS in 13 TeV data", *JINST* **15** (2020) P09018, doi:10.1088/1748-0221/15/09/p09018, arXiv:2003.00503.

[39] D. Krohn, J. Thaler, and L.-T. Wang, "Jet trimming", *JHEP* **02** (2010) 084, doi:10.1007/JHEP02(2010)084, arXiv:0912.1342.

[40] H. Qu and L. Gouskos, "Jet tagging via particle clouds", *Phys. Rev. D* **101** (2020) 056019, doi:10.1103/PhysRevD.101.056019, arXiv:1902.08570.

[41] CMS Collaboration, "Performance of heavy-flavour jet identification in Lorentz-boosted topologies in proton-proton collisions at $\sqrt{s} = 13\,\text{TeV}$", *JINST* **20** (2025) P11006, doi:10.1088/1748-0221/20/11/P11006, arXiv:2510.10228.

[42] CMS Collaboration, "Mass regression of highly-boosted jets using graph neural networks", CMS Detector Performance Summary CMS-DP-2021-017, 2021.

[43] CMS Collaboration, "Identification of highly Lorentz-boosted heavy particles using graph neural networks and new mass decorrelation techniques", CMS Detector Performance Summary CMS-DP-2020-002, 2020.

[44] U. Ellwanger and C. Hugonie, "Benchmark planes for Higgs-to-Higgs decays in the NMSSM", *Eur. Phys. J. C* **82** (2022) 406, doi:10.1140/epjc/s10052-022-10364-3, arXiv:2203.05049.

[45] H. Qu, C. Li, and S. Qian, "Particle transformer for jet tagging", in *Proc. 39th Int. Conf. on Machine Learning*, K. Chaudhuri et al., eds., volume 162, p. 18281. 2022. arXiv:2202.03772.

[46] CMS Collaboration, "Particle transformers for identifying Lorentz-boosted Higgs bosons decaying to a pair of W bosons", CMS Physics Analysis Summary CMS-PAS-JME-25-001, 2025.

[47] CMS Collaboration, "Search for a massive resonance decaying to a pair of Higgs bosons in the four b quark final state in proton-proton collisions at $\sqrt{s} = 13\,\text{TeV}$", *Phys. Lett. B* **781** (2018) 244, doi:10.1016/j.physletb.2018.03.084, arXiv:1710.04960.

[48] CMS Collaboration, "Search for production of Higgs boson pairs in the four b quark final state using large-area jets in proton-proton collisions at $\sqrt{s} = 13\,\text{TeV}$", *JHEP* **01** (2019) 040, doi:10.1007/JHEP01(2019)040, arXiv:1808.01473.

[49] CMS Collaboration, "Inclusive search for highly boosted Higgs bosons decaying to bottom quark-antiquark pairs in proton-proton collisions at $\sqrt{s} = 13\,\text{TeV}$", *JHEP* **12** (2020) 85, doi:10.1007/JHEP12(2020)085, arXiv:2006.13251.

[50] S. N. Bernstein, "Démonstration du théorème de Weierstrass fondée sur le calcul des probabilités", *Comm. Soc. Math. de Kharkov* **13** (1912) 1.

[51] R. A. Fisher, "On the interpretation of χ^2 from contingency tables, and the calculation of p", *J. Royal Stat. Soc.* **85** (1922) 87, doi:10.2307/2340521.

[52] S. Baker and R. D. Cousins, "Clarification of the Use of Chi Square and Likelihood Functions in Fits to Histograms", *Nucl. Instrum. Meth. A* **221** (1984) 437, doi:10.1016/0167-5087(84)90016-4.

[53] G. Cowan, K. Cranmer, E. Gross, and O. Vitells, "Asymptotic formulae for likelihood-based tests of new physics", *Eur. Phys. J. C* **71** (2011) 1554, doi:10.1140/epjc/s10052-011-1554-0, arXiv:1007.1727. [Erratum: doi:10.1140/epjc/s10052-013-2501-z].

[54] CMS Collaboration, "The CMS statistical analysis and combination tool: COMBINE", *Comput. Softw. Big Sci.* **8** (2024) 19, doi:10.1007/s41781-024-00121-4, arXiv:2404.06614.

[55] F. A. Dreyer, G. P. Salam, and G. Soyez, "The Lund jet plane", *JHEP* **12** (2018) 064, doi:10.1007/JHEP12(2018)064, arXiv:1807.04758.

[56] CMS Collaboration, "A method for correcting the substructure of multiprong jets using the Lund jet plane", *JHEP* **11** (2025) 038, doi:10.1007/JHEP11(2025)038, arXiv:2507.07775.

[57] CMS Collaboration, "Jet energy scale and resolution measurement with Run 2 legacy data collected by CMS at 13 TeV", CMS Detector Performance Summary CMS-DP-2021-033, 2021.

[58] CMS Collaboration, "Search for nonresonant pair production of highly energetic Higgs bosons decaying to bottom quarks", *Phys. Rev. Lett.* **131** (2023) 041803, doi:10.1103/PhysRevLett.131.041803, arXiv:2205.06667.

[59] W. Verkerke and D. P. Kirkby, "The RooFit toolkit for data modeling", in *Proceedings of the 13th International Conference for Computing in High-Energy and Nuclear Physics (CHEP03)*. 2003. arXiv:physics/0306116. [eConf C0303241, MOLT007].

[60] L. Moneta et al., "The RooStats Project", *PoS* **ACAT2010** (2010) 057, doi:10.22323/1.093.0057, arXiv:1009.1003.

[61] ATLAS and CMS Collaborations, and LHC Higgs Combination Group, "Procedure for the LHC Higgs boson search combination in Summer 2011", Technical Report CMS-NOTE-2011-005, ATL-PHYS-PUB-2011-11, 2011.

[62] T. Junk, "Confidence level computation for combining searches with small statistics", *Nucl. Instrum. Meth. A* **434** (1999) 435, doi:10.1016/S0168-9002(99)00498-2, arXiv:hep-ex/9902006.

[63] A. L. Read, "Presentation of search results: The CL_s technique", *J. Phys. G* **28** (2002) 2693, doi:10.1088/0954-3899/28/10/313.

A The CMS Collaboration

Yerevan Physics Institute, Yerevan, Armenia
A. Hayrapetyan, V. Makarenko, A. Tumasyan[1]

Institut für Hochenergiephysik, Vienna, Austria
W. Adam, J.W. Andrejkovic, L. Benato, T. Bergauer, M. Dragicevic, C. Giordano, P.S. Hussain, M. Jeitler[2], N. Krammer, A. Li, D. Liko, M. Matthewman, I. Mikulec, J. Schieck[2], R. Schöfbeck[2], D. Schwarz, M. Shooshtari, M. Sonawane, W. Waltenberger, C.-E. Wulz[2]

Universiteit Antwerpen, Antwerpen, Belgium
T. Janssen, H. Kwon, D. Ocampo Henao, T. Van Laer, P. Van Mechelen

Vrije Universiteit Brussel, Brussel, Belgium
J. Bierkens, N. Breugelmans, J. D'Hondt, S. Dansana, A. De Moor, M. Delcourt, F. Heyen, Y. Hong, P. Kashko, S. Lowette, I. Makarenko, D. Müller, J. Song, S. Tavernier, M. Tytgat[3], G.P. Van Onsem, S. Van Putte, D. Vannerom

Université Libre de Bruxelles, Bruxelles, Belgium
B. Bilin, B. Clerbaux, A.K. Das, I. De Bruyn, G. De Lentdecker, H. Evard, L. Favart, P. Gianneios, A. Khalilzadeh, F.A. Khan, A. Malara, M.A. Shahzad, L. Thomas, M. Vanden Bemden, C. Vander Velde, P. Vanlaer, F. Zhang

Ghent University, Ghent, Belgium
M. De Coen, D. Dobur, G. Gokbulut, J. Knolle, D. Marckx, K. Skovpen, A.M. Tomaru, N. Van Den Bossche, J. van der Linden, J. Vandenbroeck, L. Wezenbeek

Université Catholique de Louvain, Louvain-la-Neuve, Belgium
S. Bein, A. Benecke, A. Bethani, G. Bruno, A. Cappati, J. De Favereau De Jeneret, C. Delaere, F. Gameiro Casalinho, A. Giammanco, A.O. Guzel, V. Lemaitre, J. Lidrych, P. Malek, P. Mastrapasqua, S. Turkcapar

Centro Brasileiro de Pesquisas Fisicas, Rio de Janeiro, Brazil
G.A. Alves, M. Barroso Ferreira Filho, E. Coelho, C. Hensel, T. Menezes De Oliveira, C. Mora Herrera, P. Rebello Teles, M. Soeiro, E.J. Tonelli Manganote[4], A. Vilela Pereira[5]

Universidade do Estado do Rio de Janeiro, Rio de Janeiro, Brazil
W.L. Aldá Júnior, H. Brandao Malbouisson, W. Carvalho, J. Chinellato[6], M. Costa Reis, E.M. Da Costa, G.G. Da Silveira[7], D. De Jesus Damiao, S. Fonseca De Souza, R. Gomes De Souza, S. S. Jesus, T. Laux Kuhn[7], M. Macedo, K. Mota Amarilo, L. Mundim, H. Nogima, J.P. Pinheiro, A. Santoro, A. Sznajder, M. Thiel, F. Torres Da Silva De Araujo[8]

Universidade Estadual Paulista, Universidade Federal do ABC, São Paulo, Brazil
C.A. Bernardes[7], F. Damas, T.R. Fernandez Perez Tomei, E.M. Gregores, B. Lopes Da Costa, I. Maietto Silverio, P.G. Mercadante, S.F. Novaes, B. Orzari, Sandra S. Padula, V. Scheurer

Institute for Nuclear Research and Nuclear Energy, Bulgarian Academy of Sciences, Sofia, Bulgaria
A. Aleksandrov, G. Antchev, P. Danev, R. Hadjiiska, P. Iaydjiev, M. Shopova, G. Sultanov

University of Sofia, Sofia, Bulgaria
A. Dimitrov, L. Litov, B. Pavlov, P. Petkov, A. Petrov

Instituto De Alta Investigación, Universidad de Tarapacá, Casilla 7 D, Arica, Chile
S. Keshri, D. Laroze, S. Thakur

Universidad Tecnica Federico Santa Maria, Valparaiso, Chile
W. Brooks

Beihang University, Beijing, China
T. Cheng, T. Javaid, L. Wang, L. Yuan

Department of Physics, Tsinghua University, Beijing, China
Z. Hu, Z. Liang, J. Liu, X. Wang, H. Yang

Institute of High Energy Physics, Beijing, China
G.M. Chen[9], H.S. Chen[9], M. Chen[9], Y. Chen, Q. Hou, X. Hou, F. Iemmi, C.H. Jiang, A. Kapoor[10], H. Liao, G. Liu, Z.-A. Liu[11], J.N. Song[11], S. Song, J. Tao, C. Wang[9], J. Wang, H. Zhang, J. Zhao

State Key Laboratory of Nuclear Physics and Technology, Peking University, Beijing, China
A. Agapitos, Y. Ban, A. Carvalho Antunes De Oliveira, S. Deng, B. Guo, Q. Guo, C. Jiang, A. Levin, C. Li, Q. Li, Y. Mao, S. Qian, S.J. Qian, X. Qin, C. Quaranta, X. Sun, D. Wang, J. Wang, M. Zhang, Y. Zhao, C. Zhou

State Key Laboratory of Nuclear Physics and Technology, Institute of Quantum Matter, South China Normal University, Guangzhou, China
S. Yang

Sun Yat-Sen University, Guangzhou, China
Z. You

University of Science and Technology of China, Hefei, China
K. Jaffel, N. Lu

Nanjing Normal University, Nanjing, China
G. Bauer[12,13], Z. Cui[13], B. Li[14], H. Wang, K. Yi[15], J. Zhang

Institute of Modern Physics and Key Laboratory of Nuclear Physics and Ion-beam Application (MOE) - Fudan University, Shanghai, China
Y. Li

Zhejiang University, Hangzhou, Zhejiang, China
Z. Lin, C. Lu, M. Xiao[16]

Universidad de Los Andes, Bogota, Colombia
C. Avila, D.A. Barbosa Trujillo, A. Cabrera, C. Florez, J. Fraga, J.A. Reyes Vega

Universidad de Antioquia, Medellin, Colombia
C. Rendón, M. Rodriguez, A.A. Ruales Barbosa, J.D. Ruiz Alvarez

University of Split, Faculty of Electrical Engineering, Mechanical Engineering and Naval Architecture, Split, Croatia
N. Godinovic, D. Lelas, A. Sculac

University of Split, Faculty of Science, Split, Croatia
M. Kovac, A. Petkovic, T. Sculac

Institute Rudjer Boskovic, Zagreb, Croatia
P. Bargassa, V. Brigljevic, B.K. Chitroda, D. Ferencek, K. Jakovcic, A. Starodumov, T. Susa

University of Cyprus, Nicosia, Cyprus
A. Attikis, K. Christoforou, C. Leonidou, C. Nicolaou, L. Paizanos, F. Ptochos, P.A. Razis, H. Rykaczewski, H. Saka, A. Stepennov

Charles University, Prague, Czech Republic
M. Finger[†], M. Finger Jr.

Escuela Politecnica Nacional, Quito, Ecuador
E. Ayala

Universidad San Francisco de Quito, Quito, Ecuador
E. Carrera Jarrin

Academy of Scientific Research and Technology of the Arab Republic of Egypt, Egyptian Network of High Energy Physics, Cairo, Egypt
S. Khalil[17], E. Salama[18,19]

Center for High Energy Physics (CHEP-FU), Fayoum University, El-Fayoum, Egypt
A. Hussein, H. Mohammed

National Institute of Chemical Physics and Biophysics, Tallinn, Estonia
K. Ehataht, M. Kadastik, T. Lange, C. Nielsen, J. Pata, M. Raidal, N. Seeba, L. Tani

Department of Physics, University of Helsinki, Helsinki, Finland
E. Brücken, A. Milieva, K. Osterberg, M. Voutilainen

Helsinki Institute of Physics, Helsinki, Finland
F. Garcia, P. Inkaew, K.T.S. Kallonen, R. Kumar Verma, T. Lampén, K. Lassila-Perini, B. Lehtela, S. Lehti, T. Lindén, N.R. Mancilla Xinto, M. Myllymäki, M.m. Rantanen, S. Saariokari, N.T. Toikka, J. Tuominiemi

Lappeenranta-Lahti University of Technology, Lappeenranta, Finland
N. Bin Norjoharuddeen, H. Kirschenmann, P. Luukka, H. Petrow

IRFU, CEA, Université Paris-Saclay, Gif-sur-Yvette, France
M. Besancon, F. Couderc, M. Dejardin, D. Denegri, P. Devouge, J.L. Faure, F. Ferri, P. Gaigne, S. Ganjour, P. Gras, G. Hamel de Monchenault, M. Kumar, V. Lohezic, Y. Maidannyk, J. Malcles, F. Orlandi, L. Portales, S. Ronchi, M.Ö. Sahin, A. Savoy-Navarro[20], P. Simkina, M. Titov, M. Tornago

Laboratoire Leprince-Ringuet, CNRS/IN2P3, Ecole Polytechnique, Institut Polytechnique de Paris, Palaiseau, France
R. Amella Ranz, F. Beaudette, G. Boldrini, P. Busson, C. Charlot, M. Chiusi, T.D. Cuisset, O. Davignon, A. De Wit, T. Debnath, I.T. Ehle, S. Ghosh, A. Gilbert, R. Granier de Cassagnac, L. Kalipoliti, M. Manoni, M. Nguyen, S. Obraztsov, C. Ochando, R. Salerno, J.B. Sauvan, Y. Sirois, G. Sokmen, L. Urda Gómez, A. Zabi, A. Zghiche

Université de Strasbourg, CNRS, IPHC UMR 7178, Strasbourg, France
J.-L. Agram[21], J. Andrea, D. Bloch, J.-M. Brom, E.C. Chabert, C. Collard, G. Coulon, S. Falke, U. Goerlach, R. Haeberle, A.-C. Le Bihan, M. Meena,

O. Poncet, G. Saha, P. Vaucelle

Centre de Calcul de l'Institut National de Physique Nucleaire et de Physique des Particules, CNRS/IN2P3, Villeurbanne, France
A. Di Florio

Institut de Physique des 2 Infinis de Lyon (IP2I), Villeurbanne, France
D. Amram, S. Beauceron, B. Blancon, G. Boudoul, N. Chanon, D. Contardo, P. Depasse, H. El Mamouni, J. Fay, S. Gascon, M. Gouzevitch, C. Greenberg, G. Grenier, B. Ille, E. Jourd'Huy, M. Lethuillier, B. Massoteau, L. Mirabito, A. Purohit, M. Vander Donckt, J. Xiao

Georgian Technical University, Tbilisi, Georgia
I. Bagaturia[22], I. Lomidze, Z. Tsamalaidze[23]

RWTH Aachen University, I. Physikalisches Institut, Aachen, Germany
V. Botta, S. Consuegra Rodríguez, L. Feld, K. Klein, M. Lipinski, D. Meuser, P. Nattland, V. Oppenländer, A. Pauls, D. Pérez Adán, N. Röwert, M. Teroerde

RWTH Aachen University, III. Physikalisches Institut A, Aachen, Germany
C. Daumann, S. Diekmann, A. Dodonova, N. Eich, D. Eliseev, F. Engelke, J. Erdmann, M. Erdmann, B. Fischer, T. Hebbeker, K. Hoepfner, F. Ivone, A. Jung, N. Kumar, M.y. Lee, F. Mausolf, M. Merschmeyer, A. Meyer, F. Nowotny, A. Pozdnyakov, W. Redjeb, H. Reithler, U. Sarkar, V. Sarkisovi, A. Schmidt, C. Seth, A. Sharma, J.L. Spah, V. Vaulin, S. Zaleski

RWTH Aachen University, III. Physikalisches Institut B, Aachen, Germany
M.R. Beckers, C. Dziwok, G. Flügge, N. Hoeflich, T. Kress, A. Nowack, O. Pooth, A. Stahl, A. Zotz

Deutsches Elektronen-Synchrotron, Hamburg, Germany
H. Aarup Petersen, A. Abel, M. Aldaya Martin, J. Alimena, S. Amoroso, Y. An, I. Andreev, J. Bach, S. Baxter, M. Bayatmakou, H. Becerril Gonzalez, O. Behnke, A. Belvedere, F. Blekman[24], K. Borras[25], A. Campbell, S. Chatterjee, L.X. Coll Saravia, G. Eckerlin, D. Eckstein, E. Gallo[24], A. Geiser, V. Guglielmi, M. Guthoff, A. Hinzmann, L. Jeppe, M. Kasemann, C. Kleinwort, R. Kogler, M. Komm, D. Krücker, W. Lange, D. Leyva Pernia, K.-Y. Lin, K. Lipka[26], W. Lohmann[27], J. Malvaso, R. Mankel, I.-A. Melzer-Pellmann, M. Mendizabal Morentin, A.B. Meyer, G. Milella, K. Moral Figueroa, A. Mussgiller, L.P. Nair, J. Niedziela, A. Nürnberg, J. Park, E. Ranken, A. Raspereza, D. Rastorguev, L. Rygaard, M. Scham[28,25], S. Schnake[25], P. Schütze, C. Schwanenberger[24], D. Selivanova, K. Sharko, M. Shchedrolosiev, D. Stafford, M. Torkian, F. Vazzoler, A. Ventura Barroso, R. Walsh, D. Wang, Q. Wang, K. Wichmann, L. Wiens[25], C. Wissing, Y. Yang, S. Zakharov, A. Zimermmane Castro Santos

University of Hamburg, Hamburg, Germany
A.R. Alves Andrade, M. Antonello, S. Bollweg, M. Bonanomi, K. El Morabit, Y. Fischer, M. Frahm, E. Garutti, A. Grohsjean, A.A. Guvenli, J. Haller, D. Hundhausen, G. Kasieczka, P. Keicher, R. Klanner, W. Korcari, T. Kramer, C.c. Kuo, F. Labe, J. Lange, A. Lobanov, L. Moureaux, A. Nigamova, K. Nikolopoulos, A. Paasch, K.J. Pena Rodriguez, N. Prouvost, B. Raciti, M. Rieger, D. Savoiu, P. Schleper, M. Schröder, J. Schwandt, M. Sommerhalder, H. Stadie,

G. Steinbrück, R. Ward, B. Wiederspan, M. Wolf

Karlsruher Institut fuer Technologie, Karlsruhe, Germany
S. Brommer, E. Butz, Y.M. Chen, T. Chwalek, A. Dierlamm, G.G. Dincer, U. Elicabuk, N. Faltermann, M. Giffels, A. Gottmann, F. Hartmann[29], M. Horzela, F. Hummer, U. Husemann, J. Kieseler, M. Klute, R. Kunnilan Muhammed Rafeek, O. Lavoryk, J.M. Lawhorn, A. Lintuluoto, S. Maier, M. Mormile, Th. Müller, E. Pfeffer, M. Presilla, G. Quast, K. Rabbertz, B. Regnery, R. Schmieder, N. Shadskiy, I. Shvetsov, H.J. Simonis, L. Sowa, L. Stockmeier, K. Tauqeer, M. Toms, B. Topko, N. Trevisani, C. Verstege, T. Voigtländer, R.F. Von Cube, J. Von Den Driesch, M. Wassmer, R. Wolf, W.D. Zeuner, X. Zuo

Institute of Nuclear and Particle Physics (INPP), NCSR Demokritos, Aghia Paraskevi, Greece
G. Anagnostou, G. Daskalakis, A. Kyriakis

National and Kapodistrian University of Athens, Athens, Greece
G. Melachroinos, Z. Painesis, I. Paraskevas, N. Saoulidou, K. Theofilatos, E. Tziaferi, E. Tzovara, K. Vellidis, I. Zisopoulos

National Technical University of Athens, Athens, Greece
T. Chatzistavrou, G. Karapostoli, K. Kousouris, E. Siamarkou, G. Tsipolitis

University of Ioánnina, Ioánnina, Greece
I. Bestintzanos, I. Evangelou, C. Foudas, P. Katsoulis, P. Kokkas, P.G. Kosmoglou Kioseoglou, N. Manthos, I. Papadopoulos, J. Strologas

HUN-REN Wigner Research Centre for Physics, Budapest, Hungary
D. Druzhkin, C. Hajdu, D. Horvath[30,31], K. Márton, A.J. Rádl[32], F. Sikler, V. Veszpremi

MTA-ELTE Lendület CMS Particle and Nuclear Physics Group, Eötvös Loránd University, Budapest, Hungary
M. Csanád, K. Farkas, A. Fehérkuti[33], M.M.A. Gadallah[34], Á. Kadlecsik, M. León Coello, G. Pásztor, G.I. Veres

Faculty of Informatics, University of Debrecen, Debrecen, Hungary
B. Ujvari, G. Zilizi

HUN-REN ATOMKI - Institute of Nuclear Research, Debrecen, Hungary
G. Bencze, S. Czellar, J. Molnar, Z. Szillasi

Karoly Robert Campus, MATE Institute of Technology, Gyongyos, Hungary
T. Csorgo[33], F. Nemes[33], T. Novak, I. Szanyi[35]

Panjab University, Chandigarh, India
S. Bansal, S.B. Beri, V. Bhatnagar, G. Chaudhary, S. Chauhan, N. Dhingra[36], A. Kaur, A. Kaur, H. Kaur, M. Kaur, S. Kumar, T. Sheokand, J.B. Singh, A. Singla

University of Delhi, Delhi, India
A. Bhardwaj, A. Chhetri, B.C. Choudhary, A. Kumar, A. Kumar, M. Naimuddin, S. Phor, K. Ranjan, M.K. Saini

Indian Institute of Technology Mandi (IIT-Mandi), Himachal Pradesh, India
P. Palni

University of Hyderabad, Hyderabad, India
S. Acharya[37], B. Gomber

Indian Institute of Technology Kanpur, Kanpur, India
S. Mukherjee

Saha Institute of Nuclear Physics, HBNI, Kolkata, India
S. Bhattacharya, S. Das Gupta, S. Dutta, S. Dutta, S. Sarkar

Indian Institute of Technology Madras, Madras, India
M.M. Ameen, P.K. Behera, S. Chatterjee, G. Dash, A. Dattamunsi, P. Jana, P. Kalbhor, S. Kamble, J.R. Komaragiri[38], T. Mishra, P.R. Pujahari, A.K. Sikdar, R.K. Singh, P. Verma, S. Verma, A. Vijay

IISER Mohali, India, Mohali, India
B.K. Sirasva

Tata Institute of Fundamental Research-A, Mumbai, India
L. Bhatt, S. Dugad, G.B. Mohanty, M. Shelake, P. Suryadevara

Tata Institute of Fundamental Research-B, Mumbai, India
A. Bala, S. Banerjee, S. Barman[39], R.M. Chatterjee, M. Guchait, Sh. Jain, A. Jaiswal, B.M. Joshi, S. Kumar, M. Maity[39], G. Majumder, K. Mazumdar, S. Parolia, R. Saxena, A. Thachayath

National Institute of Science Education and Research, An OCC of Homi Bhabha National Institute, Bhubaneswar, Odisha, India
S. Bahinipati[40], D. Maity[41], P. Mal, K. Naskar[41], A. Nayak[41], S. Nayak, K. Pal, R. Raturi, P. Sadangi, S.K. Swain, S. Varghese[41], D. Vats[41]

Indian Institute of Science Education and Research (IISER), Pune, India
A. Alpana, S. Dube, P. Hazarika, B. Kansal, A. Laha, R. Sharma, S. Sharma, K.Y. Vaish

Indian Institute of Technology Hyderabad, Telangana, India
S. Ghosh

Isfahan University of Technology, Isfahan, Iran
H. Bakhshiansohi[42], A. Jafari[43], V. Sedighzadeh Dalavi, M. Zeinali[44]

Institute for Research in Fundamental Sciences (IPM), Tehran, Iran
S. Bashiri, S. Chenarani[45], S.M. Etesami, Y. Hosseini, M. Khakzad, E. Khazaie, M. Mohammadi Najafabadi, S. Tizchang[46]

University College Dublin, Dublin, Ireland
M. Felcini, M. Grunewald

INFN Sezione di Bari[a], Università di Bari[b], Politecnico di Bari[c], Bari, Italy
M. Abbrescia[a,b], M. Barbieri[a,b], M. Buonsante[a,b], A. Colaleo[a,b], D. Creanza[a,c], N. De Filippis[a,c], M. De Palma[a,b], W. Elmetenawee[a,b,47], N. Ferrara[a,c], L. Fiore[a], L. Longo[a], M. Louka[a,b], G. Maggi[a,c], M. Maggi[a], I. Margjeka[a], V. Mastrapasqua[a,b], S. My[a,b], F. Nenna[a,b], S. Nuzzo[a,b], A. Pellecchia[a,b], A. Pompili[a,b], G. Pugliese[a,c], R. Radogna[a,b], D. Ramos[a], A. Ranieri[a], L. Silvestris[a], F.M. Simone[a,c], Ü. Sözbilir[a], A. Stamerra[a,b], D. Troiano[a,b], R. Venditti[a,b], P. Verwilligen[a], A. Zaza[a,b]

INFN Sezione di Bologna[a], Università di Bologna[b], Bologna, Italy
G. Abbiendi[a], C. Battilana[a,b], D. Bonacorsi[a,b], P. Capiluppi[a,b], F.R. Cavallo[a], M. Cuffiani[a,b], T. Diotalevi[a,b], F. Fabbri[a], A. Fanfani[a,b], D. Fasanella[a], P. Giacomelli[a], L. Giommi[a,b], L. Guiducci[a,b], S. Lo Meo[a,48], M. Lorusso[a,b], L. Lunerti[a], S. Marcellini[a], G. Masetti[a], F.L. Navarria[a,b], G. Paggi[a,b], A. Perrotta[a], F. Primavera[a,b], A.M. Rossi[a,b], S. Rossi Tisbeni[a,b], T. Rovelli[a,b], G.P. Siroli[a,b]

INFN Sezione di Catania[a], Università di Catania[b], Catania, Italy
S. Costa[a,b,49], A. Di Mattia[a], A. Lapertosa[a], R. Potenza[a,b], A. Tricomi[a,b,49]

INFN Sezione di Firenze[a], Università di Firenze[b], Firenze, Italy
J. Altork[a,b], P. Assiouras[a], G. Barbagli[a], G. Bardelli[a], M. Bartolini[a,b], A. Calandri[a,b], B. Camaiani[a,b], A. Cassese[a], R. Ceccarelli[a], V. Ciulli[a,b], C. Civinini[a], R. D'Alessandro[a,b], L. Damenti[a,b], E. Focardi[a,b], T. Kello[a], G. Latino[a,b], P. Lenzi[a,b], M. Lizzo[a], M. Meschini[a], S. Paoletti[a], A. Papanastassiou[a,b], G. Sguazzoni[a], L. Viliani[a]

INFN Laboratori Nazionali di Frascati, Frascati, Italy
L. Benussi, S. Bianco, S. Meola[50], D. Piccolo

INFN Sezione di Genova[a], Università di Genova[b], Genova, Italy
M. Alves Gallo Pereira[a], F. Ferro[a], E. Robutti[a], S. Tosi[a,b]

INFN Sezione di Milano-Bicocca[a], Università di Milano-Bicocca[b], Milano, Italy
A. Benaglia[a], F. Brivio[a], V. Camagni[a,b], F. Cetorelli[a,b], F. De Guio[a,b], M.E. Dinardo[a,b], P. Dini[a], S. Gennai[a], R. Gerosa[a,b], A. Ghezzi[a,b], P. Govoni[a,b], L. Guzzi[a], M.R. Kim[a], G. Lavizzari[a,b], M.T. Lucchini[a,b], M. Malberti[a], S. Malvezzi[a], A. Massironi[a], D. Menasce[a], L. Moroni[a], M. Paganoni[a,b], S. Palluotto[a,b], D. Pedrini[a], A. Perego[a,b], G. Pizzati[a,b], T. Tabarelli de Fatis[a,b]

INFN Sezione di Napoli[a], Università di Napoli 'Federico II'[b], Napoli, Italy; Università della Basilicata[c], Potenza, Italy; Scuola Superiore Meridionale (SSM)[d], Napoli, Italy
S. Buontempo[a], C. Di Fraia[a,b], F. Fabozzi[a,c], L. Favilla[a,d], A.O.M. Iorio[a,b], L. Lista[a,b,51], P. Paolucci[a,29], B. Rossi[a]

INFN Sezione di Padova[a], Università di Padova[b], Padova, Italy; Universita degli Studi di Cagliari[c], Cagliari, Italy
P. Azzi[a], N. Bacchetta[a,52], P. Bortignon[a,c], G. Bortolato[a,b], A.C.M. Bulla[a,c], R. Carlin[a,b], P. Checchia[a], T. Dorigo[a,53], F. Gasparini[a,b], U. Gasparini[a,b], S. Giorgetti[a], F. Gonella[a], E. Lusiani[a], M. Margoni[a,b], A.T. Meneguzzo[a,b], J. Pazzini[a,b], P. Ronchese[a,b], R. Rossin[a,b], M. Tosi[a,b], A. Triossi[a,b], S. Ventura[a], M. Zanetti[a,b], P. Zotto[a,b], A. Zucchetta[a,b], G. Zumerle[a,b]

INFN Sezione di Pavia[a], Università di Pavia[b], Pavia, Italy
A. Braghieri[a], S. Calzaferri[a], P. Montagna[a,b], M. Pelliccioni[a], V. Re[a], C. Riccardi[a,b], P. Salvini[a], I. Vai[a,b], P. Vitulo[a,b]

INFN Sezione di Perugia[a], Università di Perugia[b], Perugia, Italy
S. Ajmal[a,b], M.E. Ascioti[a,b], G.M. Bilei[†a], C. Carrivale[a,b], D. Ciangottini[a,b], L. Della Penna[a,b], L. Fanò[a,b], V. Mariani[a,b], M. Menichelli[a], F. Moscatelli[a,54], A. Rossi[a,b], A. Santocchia[a,b], D. Spiga[a], T. Tedeschi[a,b]

INFN Sezione di Pisa[a], Università di Pisa[b], Scuola Normale Superiore di Pisa[c], Pisa, Italy;

Università di Siena[d], Siena, Italy
C. Aimè[a,b], C.A. Alexe[a,c], P. Asenov[a,b], P. Azzurri[a], G. Bagliesi[a], L. Bianchini[a,b], T. Boccali[a], E. Bossini[a], D. Bruschini[a,c], L. Calligaris[a,b], R. Castaldi[a], F. Cattafesta[a,c], M.A. Ciocci[a,d], M. Cipriani[a,b], R. Dell'Orso[a], S. Donato[a,b], R. Forti[a,b], A. Giassi[a], F. Ligabue[a,c], A.C. Marini[a,b], D. Matos Figueiredo[a], A. Messineo[a,b], S. Mishra[a], V.K. Muraleedharan Nair Bindhu[a,b], S. Nandan[a], F. Palla[a], M. Riggirello[a,c], A. Rizzi[a,b], G. Rolandi[a,c], S. Roy Chowdhury[a,55], T. Sarkar[a], A. Scribano[a], P. Solanki[a,b], P. Spagnolo[a], F. Tenchini[a,b], R. Tenchini[a], G. Tonelli[a,b], N. Turini[a,d], F. Vaselli[a,c], A. Venturi[a], P.G. Verdini[a]

INFN Sezione di Roma[a], Sapienza Università di Roma[b], Roma, Italy
P. Akrap[a,b], C. Basile[a,b], S.C. Behera[a], F. Cavallari[a], L. Cunqueiro Mendez[a,b], F. De Riggi[a,b], D. Del Re[a,b], E. Di Marco[a], M. Diemoz[a], F. Errico[a], L. Frosina[a,b], R. Gargiulo[a,b], B. Harikrishnan[a,b], F. Lombardi[a,b], E. Longo[a,b], L. Martikainen[a,b], J. Mijuskovic[a,b], G. Organtini[a,b], N. Palmeri[a,b], R. Paramatti[a,b], S. Rahatlou[a,b], C. Rovelli[a], F. Santanastasio[a,b], L. Soffi[a], V. Vladimirov[a,b]

INFN Sezione di Torino[a], Università di Torino[b], Torino, Italy; Università del Piemonte Orientale[c], Novara, Italy
N. Amapane[a,b], R. Arcidiacono[a,c], S. Argiro[a,b], M. Arneodo[a,c], N. Bartosik[a,c], R. Bellan[a,b], A. Bellora[a,b], C. Biino[a], C. Borca[a,b], N. Cartiglia[a], M. Costa[a,b], R. Covarelli[a,b], N. Demaria[a], L. Finco[a], M. Grippo[a,b], B. Kiani[a,b], L. Lanteri[a,b], F. Legger[a], F. Luongo[a,b], C. Mariotti[a], S. Maselli[a], A. Mecca[a,b], L. Menzio[a,b], P. Meridiani[a], E. Migliore[a,b], M. Monteno[a], M.M. Obertino[a,b], G. Ortona[a], L. Pacher[a,b], N. Pastrone[a], M. Ruspa[a,c], F. Siviero[a,b], V. Sola[a,b], A. Solano[a,b], A. Staiano[a], C. Tarricone[a,b], D. Trocino[a], G. Umoret[a,b], E. Vlasov[a,b], R. White[a,b]

INFN Sezione di Trieste[a], Università di Trieste[b], Trieste, Italy
J. Babbar[a,b], S. Belforte[a], V. Candelise[a,b], M. Casarsa[a], F. Cossutti[a], K. De Leo[a], G. Della Ricca[a,b], R. Delli Gatti[a,b]

Kyungpook National University, Daegu, Korea
S. Dogra, J. Hong, J. Kim, T. Kim, D. Lee, H. Lee, J. Lee, S.W. Lee, C.S. Moon, Y.D. Oh, S. Sekmen, B. Tae, Y.C. Yang

Department of Mathematics and Physics - GWNU, Gangneung, Korea
M.S. Kim

Chonnam National University, Institute for Universe and Elementary Particles, Kwangju, Korea
G. Bak, P. Gwak, H. Kim, D.H. Moon, J. Seo

Hanyang University, Seoul, Korea
E. Asilar, F. Carnevali, J. Choi[56], T.J. Kim, Y. Ryou

Korea University, Seoul, Korea
S. Ha, S. Han, B. Hong, J. Kim, K. Lee, K.S. Lee, S. Lee, J. Yoo

Kyung Hee University, Department of Physics, Seoul, Korea
J. Goh, J. Shin, S. Yang

Sejong University, Seoul, Korea
Y. Kang, H. S. Kim, Y. Kim, S. Lee

Seoul National University, Seoul, Korea

J. Almond, J.H. Bhyun, J. Choi, J. Choi, W. Jun, H. Kim, J. Kim, T. Kim, Y. Kim, Y.W. Kim, S. Ko, H. Lee, J. Lee, J. Lee, B.H. Oh, S.B. Oh, J. Shin, U.K. Yang, I. Yoon

University of Seoul, Seoul, Korea
W. Jang, D.Y. Kang, D. Kim, S. Kim, B. Ko, J.S.H. Lee, Y. Lee, I.C. Park, Y. Roh, I.J. Watson

Yonsei University, Department of Physics, Seoul, Korea
G. Cho, K. Hwang, B. Kim, S. Kim, K. Lee, H.D. Yoo

Sungkyunkwan University, Suwon, Korea
Y. Lee, I. Yu

College of Engineering and Technology, American University of the Middle East (AUM), Dasman, Kuwait
T. Beyrouthy, Y. Gharbia

Kuwait University - College of Science - Department of Physics, Safat, Kuwait
F. Alazemi

Riga Technical University, Riga, Latvia
K. Dreimanis, O.M. Eberlins, A. Gaile, C. Munoz Diaz, D. Osite, G. Pikurs, R. Plese, A. Potrebko, M. Seidel, D. Sidiropoulos Kontos

University of Latvia (LU), Riga, Latvia
N.R. Strautnieks

Vilnius University, Vilnius, Lithuania
M. Ambrozas, A. Juodagalvis, S. Nargelas, A. Rinkevicius, G. Tamulaitis

National Centre for Particle Physics, Universiti Malaya, Kuala Lumpur, Malaysia
I. Yusuff[57], Z. Zolkapli

Universidad de Sonora (UNISON), Hermosillo, Mexico
J.F. Benitez, A. Castaneda Hernandez, A. Cota Rodriguez, L.E. Cuevas Picos, H.A. Encinas Acosta, L.G. Gallegos Maríñez, J.A. Murillo Quijada, L. Valencia Palomo

Centro de Investigacion y de Estudios Avanzados del IPN, Mexico City, Mexico
G. Ayala, H. Castilla-Valdez, H. Crotte Ledesma, R. Lopez-Fernandez, J. Mejia Guisao, R. Reyes-Almanza, A. Sánchez Hernández

Universidad Iberoamericana, Mexico City, Mexico
C. Oropeza Barrera, D.L. Ramirez Guadarrama, M. Ramírez García

Benemerita Universidad Autonoma de Puebla, Puebla, Mexico
I. Bautista, F.E. Neri Huerta, I. Pedraza, H.A. Salazar Ibarguen, C. Uribe Estrada

University of Montenegro, Podgorica, Montenegro
I. Bubanja, N. Raicevic

University of Canterbury, Christchurch, New Zealand
P.H. Butler

National Centre for Physics, Quaid-I-Azam University, Islamabad, Pakistan
A. Ahmad, M.I. Asghar, A. Awais, M.I.M. Awan, W.A. Khan

AGH University of Krakow, Krakow, Poland

V. Avati, L. Forthomme, L. Grzanka, M. Malawski, K. Piotrzkowski

National Centre for Nuclear Research, Swierk, Poland
M. Bluj, M. Górski, M. Kazana, M. Szleper, P. Zalewski

Institute of Experimental Physics, Faculty of Physics, University of Warsaw, Warsaw, Poland
K. Bunkowski, K. Doroba, A. Kalinowski, M. Konecki, J. Krolikowski, A. Muhammad

Warsaw University of Technology, Warsaw, Poland
P. Fokow, K. Pozniak, W. Zabolotny

Laboratório de Instrumentação e Física Experimental de Partículas, Lisboa, Portugal
M. Araujo, D. Bastos, C. Beirão Da Cruz E Silva, A. Boletti, M. Bozzo, T. Camporesi, G. Da Molin, M. Gallinaro, J. Hollar, N. Leonardo, G.B. Marozzo, A. Petrilli, M. Pisano, J. Seixas, J. Varela, J.W. Wulff

Faculty of Physics, University of Belgrade, Belgrade, Serbia
P. Adzic, L. Markovic, P. Milenovic, V. Milosevic

VINCA Institute of Nuclear Sciences, University of Belgrade, Belgrade, Serbia
D. Devetak, M. Dordevic, J. Milosevic, L. Nadderd, V. Rekovic, M. Stojanovic

Centro de Investigaciones Energéticas Medioambientales y Tecnológicas (CIEMAT), Madrid, Spain
M. Alcalde Martinez, J. Alcaraz Maestre, Cristina F. Bedoya, J.A. Brochero Cifuentes, Oliver M. Carretero, M. Cepeda, M. Cerrada, N. Colino, B. De La Cruz, A. Delgado Peris, A. Escalante Del Valle, D. Fernández Del Val, J.P. Fernández Ramos, J. Flix, M.C. Fouz, M. Gonzalez Hernandez, O. Gonzalez Lopez, S. Goy Lopez, J.M. Hernandez, M.I. Josa, J. Llorente Merino, C. Martin Perez, E. Martin Viscasillas, D. Moran, C. M. Morcillo Perez, Á. Navarro Tobar, R. Paz Herrera, C. Perez Dengra, A. Pérez-Calero Yzquierdo, J. Puerta Pelayo, I. Redondo, J. Vazquez Escobar

Universidad Autónoma de Madrid, Madrid, Spain
J.F. de Trocóniz

Universidad de Oviedo, Instituto Universitario de Ciencias y Tecnologías Espaciales de Asturias (ICTEA), Oviedo, Spain
B. Alvarez Gonzalez, J. Ayllon Torresano, A. Cardini, J. Cuevas, J. Del Riego Badas, D. Estrada Acevedo, J. Fernandez Menendez, S. Folgueras, I. Gonzalez Caballero, P. Leguina, M. Obeso Menendez, E. Palencia Cortezon, J. Prado Pico, A. Soto Rodríguez, C. Vico Villalba, P. Vischia

Instituto de Física de Cantabria (IFCA), CSIC-Universidad de Cantabria, Santander, Spain
S. Blanco Fernández, I.J. Cabrillo, A. Calderon, J. Duarte Campderros, M. Fernandez, G. Gomez, C. Lasaosa García, R. Lopez Ruiz, C. Martinez Rivero, P. Martinez Ruiz del Arbol, F. Matorras, P. Matorras Cuevas, E. Navarrete Ramos, J. Piedra Gomez, C. Quintana San Emeterio, L. Scodellaro, I. Vila, R. Vilar Cortabitarte, J.M. Vizan Garcia

University of Colombo, Colombo, Sri Lanka
B. Kailasapathy[58], D.D.C. Wickramarathna

University of Ruhuna, Department of Physics, Matara, Sri Lanka

W.G.D. Dharmaratna[59], K. Liyanage, N. Perera

CERN, European Organization for Nuclear Research, Geneva, Switzerland
D. Abbaneo, C. Amendola, R. Ardino, E. Auffray, J. Baechler, D. Barney, J. Bendavid, M. Bianco, A. Bocci, L. Borgonovi, C. Botta, A. Bragagnolo, C.E. Brown, C. Caillol, G. Cerminara, P. Connor, D. d'Enterria, A. Dabrowski, A. David, A. De Roeck, M.M. Defranchis, M. Deile, M. Dobson, P.J. Fernández Manteca, B.A. Fontana Santos Alves, E. Fontanesi, W. Funk, A. Gaddi, S. Giani, D. Gigi, K. Gill, F. Glege, M. Glowacki, A. Gruber, J. Hegeman, J.K. Heikkilä, R. Hofsaess, B. Huber, T. James, P. Janot, O. Kaluzinska, O. Karacheban[27], G. Karathanasis, S. Laurila, P. Lecoq, E. Leutgeb, C. Lourenço, A.-M. Lyon, M. Magherini, L. Malgeri, M. Mannelli, A. Mehta, F. Meijers, J.A. Merlin, S. Mersi, E. Meschi, M. Migliorini, F. Monti, F. Moortgat, M. Mulders, M. Musich, I. Neutelings, S. Orfanelli, F. Pantaleo, M. Pari, G. Petrucciani, A. Pfeiffer, M. Pierini, M. Pitt, H. Qu, D. Rabady, A. Reimers, B. Ribeiro Lopes, F. Riti, P. Rosado, M. Rovere, H. Sakulin, R. Salvatico, S. Sanchez Cruz, S. Scarfi, M. Selvaggi, A. Sharma, K. Shchelina, P. Silva, P. Sphicas[60], A.G. Stahl Leiton, A. Steen, S. Summers, D. Treille, P. Tropea, E. Vernazza, J. Wanczyk[61], S. Wuchterl, M. Zarucki, P. Zehetner, P. Zejdl, G. Zevi Della Porta

PSI Center for Neutron and Muon Sciences, Villigen, Switzerland
T. Bevilacqua[62], L. Caminada[62], W. Erdmann, R. Horisberger, Q. Ingram, H.C. Kaestli, D. Kotlinski, C. Lange, U. Langenegger, L. Noehte[62], T. Rohe, A. Samalan

ETH Zurich - Institute for Particle Physics and Astrophysics (IPA), Zurich, Switzerland
T.K. Aarrestad, M. Backhaus, G. Bonomelli, C. Cazzaniga, K. Datta, P. De Bryas Dexmiers D'Archiacchiac[61], A. De Cosa, G. Dissertori, M. Dittmar, M. Donegà, F. Eble, K. Gedia, F. Glessgen, C. Grab, N. Härringer, T.G. Harte, W. Lustermann, M. Malucchi, R.A. Manzoni, L. Marchese, A. Mascellani[61], F. Nessi-Tedaldi, F. Pauss, V. Perovic, B. Ristic, R. Seidita, J. Steggemann[61], A. Tarabini, D. Valsecchi, R. Wallny

Universität Zürich, Zurich, Switzerland
C. Amsler[63], P. Bärtschi, F. Bilandzija, M.F. Canelli, G. Celotto, K. Cormier, M. Huwiler, W. Jin, A. Jofrehei, B. Kilminster, T.H. Kwok, S. Leontsinis, V. Lukashenko, A. Macchiolo, F. Meng, M. Missiroli, J. Motta, P. Robmann, M. Senger, E. Shokr, F. Stäger, R. Tramontano, P. Viscone

National Central University, Chung-Li, Taiwan
D. Bhowmik, C.M. Kuo, P.K. Rout, S. Taj, P.C. Tiwari[38]

National Taiwan University (NTU), Taipei, Taiwan
L. Ceard, K.F. Chen, Z.g. Chen, A. De Iorio, W.-S. Hou, T.h. Hsu, Y.w. Kao, S. Karmakar, G. Kole, Y.y. Li, R.-S. Lu, E. Paganis, X.f. Su, J. Thomas-Wilsker, L.s. Tsai, D. Tsionou, H.y. Wu, E. Yazgan

High Energy Physics Research Unit, Department of Physics, Faculty of Science, Chulalongkorn University, Bangkok, Thailand
C. Asawatangtrakuldee, N. Srimanobhas

Tunis El Manar University, Tunis, Tunisia
Y. Maghrbi

Çukurova University, Physics Department, Science and Art Faculty, Adana, Turkey
D. Agyel, F. Dolek, I. Dumanoglu[64], Y. Guler[65], E. Gurpinar Guler[65], C. Isik, O. Kara, A. Kayis Topaksu, Y. Komurcu, G. Onengut, K. Ozdemir[66], B. Tali[67], U.G. Tok, E. Uslan, I.S. Zorbakir

Hacettepe University, Ankara, Turkey
S. Sen

Middle East Technical University, Physics Department, Ankara, Turkey
M. Yalvac[68]

Bogazici University, Istanbul, Turkey
B. Akgun, I.O. Atakisi[69], E. Gülmez, M. Kaya[70], O. Kaya[71], M.A. Sarkisla[72], S. Tekten[73]

Istanbul Technical University, Istanbul, Turkey
D. Boncukcu, A. Cakir, K. Cankocak[64,74]

Istanbul University, Istanbul, Turkey
B. Hacisahinoglu, I. Hos[75], B. Kaynak, S. Ozkorucuklu, O. Potok, H. Sert, C. Simsek, C. Zorbilmez

Yildiz Technical University, Istanbul, Turkey
S. Cerci, C. Dozen[76], B. Isildak[77], E. Simsek, D. Sunar Cerci, T. Yetkin[76]

Institute for Scintillation Materials of National Academy of Science of Ukraine, Kharkiv, Ukraine
A. Boyaryntsev, O. Dadazhanova, B. Grynyov

National Science Centre, Kharkiv Institute of Physics and Technology, Kharkiv, Ukraine
L. Levchuk

University of Bristol, Bristol, United Kingdom
J.J. Brooke, A. Bundock, F. Bury, E. Clement, D. Cussans, D. Dharmender, H. Flacher, J. Goldstein, H.F. Heath, M.-L. Holmberg, L. Kreczko, S. Paramesvaran, L. Robertshaw, M.S. Sanjrani[42], J. Segal, V.J. Smith

Rutherford Appleton Laboratory, Didcot, United Kingdom
A.H. Ball, K.W. Bell, A. Belyaev[78], C. Brew, R.M. Brown, D.J.A. Cockerill, A. Elliot, K.V. Ellis, J. Gajownik, K. Harder, S. Harper, J. Linacre, K. Manolopoulos, M. Moallemi, D.M. Newbold, E. Olaiya, D. Petyt, T. Reis, A.R. Sahasransu, G. Salvi, T. Schuh, C.H. Shepherd-Themistocleous, I.R. Tomalin, K.C. Whalen, T. Williams

Imperial College, London, United Kingdom
I. Andreou, R. Bainbridge, P. Bloch, O. Buchmuller, C.A. Carrillo Montoya, D. Colling, I. Das, P. Dauncey, G. Davies, M. Della Negra, S. Fayer, G. Fedi, G. Hall, H.R. Hoorani, A. Howard, G. Iles, C.R. Knight, P. Krueper, J. Langford, K.H. Law, J. León Holgado, L. Lyons, A.-M. Magnan, B. Maier, S. Mallios, A. Mastronikolis, M. Mieskolainen, J. Nash[79], M. Pesaresi, P.B. Pradeep, B.C. Radburn-Smith, A. Richards, A. Rose, L. Russell, K. Savva, C. Seez, R. Shukla, A. Tapper, K. Uchida, G.P. Uttley, T. Virdee[29], M. Vojinovic, N. Wardle, D. Winterbottom

Brunel University, Uxbridge, United Kingdom

J.E. Cole, A. Khan, P. Kyberd, I.D. Reid

Baylor University, Waco, Texas, USA
S. Abdullin, A. Brinkerhoff, E. Collins, M.R. Darwish, J. Dittmann, K. Hatakeyama, V. Hegde, J. Hiltbrand, B. McMaster, J. Samudio, S. Sawant, C. Sutantawibul, J. Wilson

Bethel University, St. Paul, Minnesota, USA
J.M. Hogan

Catholic University of America, Washington, DC, USA
R. Bartek, A. Dominguez, S. Raj, B. Sahu[37], A.E. Simsek, S.S. Yu

The University of Alabama, Tuscaloosa, Alabama, USA
B. Bam, A. Buchot Perraguin, S. Campbell, R. Chudasama, S.I. Cooper, C. Crovella, G. Fidalgo, S.V. Gleyzer, A. Khukhunaishvili, K. Matchev, E. Pearson, C.U. Perez, P. Rumerio[80], E. Usai, R. Yi

Boston University, Boston, Massachusetts, USA
S. Cholak, G. De Castro, Z. Demiragli, C. Erice, C. Fangmeier, C. Fernandez Madrazo, J. Fulcher, F. Golf, S. Jeon, J. O'Cain, I. Reed, J. Rohlf, K. Salyer, D. Sperka, D. Spitzbart, I. Suarez, A. Tsatsos, E. Wurtz, A.G. Zecchinelli

Brown University, Providence, Rhode Island, USA
G. Barone, G. Benelli, D. Cutts, S. Ellis, L. Gouskos, M. Hadley, U. Heintz, K.W. Ho, T. Kwon, L. Lambrecht, G. Landsberg, K.T. Lau, J. Luo, S. Mondal, J. Roloff, T. Russell, S. Sagir[81], X. Shen, M. Stamenkovic, N. Venkatasubramanian

University of California, Davis, Davis, California, USA
S. Abbott, S. Baradia, B. Barton, R. Breedon, H. Cai, M. Calderon De La Barca Sanchez, E. Cannaert, M. Chertok, M. Citron, J. Conway, P.T. Cox, R. Erbacher, O. Kukral, G. Mocellin, S. Ostrom, I. Salazar Segovia, J.S. Tafoya Vargas, W. Wei, S. Yoo

University of California, Los Angeles, California, USA
K. Adamidis, M. Bachtis, D. Campos, R. Cousins, A. Datta, G. Flores Avila, J. Hauser, M. Ignatenko, M.A. Iqbal, T. Lam, Y.f. Lo, E. Manca, A. Nunez Del Prado, D. Saltzberg, V. Valuev

University of California, Riverside, Riverside, California, USA
R. Clare, J.W. Gary, G. Hanson

University of California, San Diego, La Jolla, California, USA
A. Aportela, A. Arora, J.G. Branson, S. Cittolin, S. Cooperstein, B. D'Anzi, D. Diaz, J. Duarte, L. Giannini, Y. Gu, J. Guiang, V. Krutelyov, R. Lee, J. Letts, H. Li, M. Masciovecchio, F. Mokhtar, S. Mukherjee, M. Pieri, D. Primosch, M. Quinnan, V. Sharma, M. Tadel, E. Vourliotis, F. Würthwein, A. Yagil, Z. Zhao

University of California, Santa Barbara - Department of Physics, Santa Barbara, California, USA
A. Barzdukas, L. Brennan, C. Campagnari, S. Carron Montero[82], K. Downham, C. Grieco, M.M. Hussain, J. Incandela, M.W.K. Lai, A.J. Li, P. Masterson, J. Richman, S.N. Santpur, U. Sarica, R. Schmitz, F. Setti, J. Sheplock, D. Stuart, T.Á. Vámi, X. Yan, D. Zhang

California Institute of Technology, Pasadena, California, USA
A. Albert, S. Bhattacharya, A. Bornheim, O. Cerri, R. Kansal, J. Mao, H.B. Newman, G. Reales Gutiérrez, T. Sievert, M. Spiropulu, J.R. Vlimant, R.A. Wynne, S. Xie

Carnegie Mellon University, Pittsburgh, Pennsylvania, USA
J. Alison, S. An, M. Cremonesi, V. Dutta, E.Y. Ertorer, T. Ferguson, T.A. Gómez Espinosa, A. Harilal, A. Kallil Tharayil, M. Kanemura, C. Liu, M. Marchegiani, P. Meiring, T. Mudholkar, S. Murthy, P. Palit, K. Park, M. Paulini, A. Roberts, A. Sanchez, W. Terrill

University of Colorado Boulder, Boulder, Colorado, USA
J.P. Cumalat, W.T. Ford, A. Hart, S. Kwan, J. Pearkes, C. Savard, N. Schonbeck, K. Stenson, K.A. Ulmer, S.R. Wagner, N. Zipper, D. Zuolo

Cornell University, Ithaca, New York, USA
J. Alexander, X. Chen, J. Dickinson, A. Duquette, J. Fan, X. Fan, J. Grassi, S. Hogan, P. Kotamnives, J. Monroy, G. Niendorf, M. Oshiro, J.R. Patterson, A. Ryd, J. Thom, P. Wittich, R. Zou, L. Zygala

Fermi National Accelerator Laboratory, Batavia, Illinois, USA
M. Albrow, M. Alyari, O. Amram, G. Apollinari, A. Apresyan, L.A.T. Bauerdick, D. Berry, J. Berryhill, P.C. Bhat, K. Burkett, J.N. Butler, A. Canepa, G.B. Cerati, H.W.K. Cheung, F. Chlebana, C. Cosby, G. Cummings, I. Dutta, V.D. Elvira, J. Freeman, A. Gandrakota, Z. Gecse, L. Gray, D. Green, A. Grummer, S. Grünendahl, D. Guerrero, O. Gutsche, R.M. Harris, T.C. Herwig, J. Hirschauer, V. Innocente, B. Jayatilaka, S. Jindariani, M. Johnson, U. Joshi, B. Klima, K.H.M. Kwok, S. Lammel, C. Lee, D. Lincoln, R. Lipton, T. Liu, K. Maeshima, D. Mason, P. McBride, P. Merkel, S. Mrenna, S. Nahn, J. Ngadiuba, D. Noonan, S. Norberg, V. Papadimitriou, N. Pastika, K. Pedro, C. Pena[83], C.E. Perez Lara, F. Ravera, A. Reinsvold Hall[84], L. Ristori, M. Safdari, E. Sexton-Kennedy, N. Smith, A. Soha, L. Spiegel, S. Stoynev, J. Strait, L. Taylor, S. Tkaczyk, N.V. Tran, L. Uplegger, E.W. Vaandering, C. Wang, I. Zoi

University of Florida, Gainesville, Florida, USA
C. Aruta, P. Avery, D. Bourilkov, P. Chang, V. Cherepanov, R.D. Field, C. Huh, E. Koenig, M. Kolosova, J. Konigsberg, A. Korytov, G. Mitselmakher, K. Mohrman, A. Muthirakalayil Madhu, N. Rawal, S. Rosenzweig, V. Sulimov, Y. Takahashi, J. Wang

Florida State University, Tallahassee, Florida, USA
T. Adams, A. Al Kadhim, A. Askew, S. Bower, R. Goff, R. Hashmi, A. Hassani, R.S. Kim, T. Kolberg, G. Martinez, M. Mazza, H. Prosper, P.R. Prova, R. Yohay

Florida Institute of Technology, Melbourne, Florida, USA
B. Alsufyani, S. Butalla, S. Das, M. Hohlmann, M. Lavinsky, E. Yanes

University of Illinois Chicago, Chicago, Illinois, USA
M.R. Adams, N. Barnett, A. Baty, C. Bennett, R. Cavanaugh, R. Escobar Franco, O. Evdokimov, C.E. Gerber, H. Gupta, M. Hawksworth, A. Hingrajiya, D.J. Hofman, Z. Huang, J.h. Lee, C. Mills, S. Nanda, G. Nigmatkulov, B. Ozek, T. Phan, D. Pilipovic, R. Pradhan, E. Prifti, P. Roy, T. Roy, N. Singh, M.B. Tonjes, N. Varelas, M.A. Wadud, J. Yoo

The University of Iowa, Iowa City, Iowa, USA

M. Alhusseini, D. Blend, K. Dilsiz[85], O.K. Köseyan, A. Mestvirishvili[86], O. Neogi, H. Ogul[87], Y. Onel, A. Penzo, C. Snyder, E. Tiras[88]

Johns Hopkins University, Baltimore, Maryland, USA
B. Blumenfeld, J. Davis, A.V. Gritsan, L. Kang, S. Kyriacou, P. Maksimovic, A. Mitra, M. Roguljic, S. Sekhar, M.V. Srivastav, M. Swartz

The University of Kansas, Lawrence, Kansas, USA
A. Abreu, L.F. Alcerro Alcerro, J. Anguiano, S. Arteaga Escatel, P. Baringer, A. Bean, R. Bhattacharya, Z. Flowers, D. Grove, J. King, G. Krintiras, M. Lazarovits, C. Le Mahieu, J. Marquez, M. Murray, M. Nickel, S. Popescu[89], C. Rogan, C. Royon, S. Rudrabhatla, S. Sanders, C. Smith, G. Wilson

Kansas State University, Manhattan, Kansas, USA
B. Allmond, N. Islam, A. Ivanov, K. Kaadze, Y. Maravin, J. Natoli, G.G. Reddy, D. Roy, G. Sorrentino

University of Maryland, College Park, Maryland, USA
A. Baden, A. Belloni, J. Bistany-riebman, S.C. Eno, N.J. Hadley, S. Jabeen, R.G. Kellogg, T. Koeth, B. Kronheim, S. Lascio, P. Major, A.C. Mignerey, C. Palmer, C. Papageorgakis, M.M. Paranjpe, E. Popova[90], A. Shevelev, L. Zhang

Massachusetts Institute of Technology, Cambridge, Massachusetts, USA
C. Baldenegro Barrera, H. Bossi, S. Bright-Thonney, I.A. Cali, Y.c. Chen, P.c. Chou, M. D'Alfonso, J. Eysermans, C. Freer, G. Gomez-Ceballos, M. Goncharov, G. Grosso, P. Harris, D. Hoang, G.M. Innocenti, K. Ivanov, D. Kovalskyi, J. Krupa, L. Lavezzo, Y.-J. Lee, K. Long, C. Mcginn, A. Novak, M.I. Park, C. Paus, C. Reissel, C. Roland, G. Roland, S. Rothman, T.a. Sheng, G.S.F. Stephans, D. Walter, J. Wang, Z. Wang, B. Wyslouch, T. J. Yang

University of Minnesota, Minneapolis, Minnesota, USA
B. Crossman, W.J. Jackson, C. Kapsiak, M. Krohn, D. Mahon, J. Mans, B. Marzocchi, R. Rusack, O. Sancar, R. Saradhy, N. Strobbe

University of Nebraska-Lincoln, Lincoln, Nebraska, USA
K. Bloom, D.R. Claes, G. Haza, J. Hossain, C. Joo, I. Kravchenko, A. Rohilla, J.E. Siado, W. Tabb, A. Vagnerini, A. Wightman, F. Yan

State University of New York at Buffalo, Buffalo, New York, USA
H. Bandyopadhyay, L. Hay, H.w. Hsia, I. Iashvili, A. Kalogeropoulos, A. Kharchilava, A. Mandal, M. Morris, D. Nguyen, S. Rappoccio, H. Rejeb Sfar, A. Williams, P. Young, D. Yu

Northeastern University, Boston, Massachusetts, USA
G. Alverson, E. Barberis, J. Bonilla, B. Bylsma, M. Campana, J. Dervan, Y. Haddad, Y. Han, I. Israr, A. Krishna, M. Lu, N. Manganelli, R. Mccarthy, D.M. Morse, T. Orimoto, L. Skinnari, C.S. Thoreson, E. Tsai, D. Wood

Northwestern University, Evanston, Illinois, USA
S. Dittmer, K.A. Hahn, M. Mcginnis, Y. Miao, D.G. Monk, M.H. Schmitt, A. Taliercio, M. Velasco, J. Wang

University of Notre Dame, Notre Dame, Indiana, USA
G. Agarwal, R. Band, R. Bucci, S. Castells, A. Das, A. Ehnis, R. Goldouzian, M. Hildreth, K. Hurtado Anampa, T. Ivanov, C. Jessop, A. Karneyeu, K. Lannon,

J. Lawrence, N. Loukas, L. Lutton, J. Mariano, N. Marinelli, I. Mcalister, T. McCauley, C. Mcgrady, C. Moore, Y. Musienko[23], H. Nelson, M. Osherson, A. Piccinelli, R. Ruchti, A. Townsend, Y. Wan, M. Wayne, H. Yockey

The Ohio State University, Columbus, Ohio, USA
A. Basnet, M. Carrigan, R. De Los Santos, L.S. Durkin, C. Hill, M. Joyce, M. Nunez Ornelas, D.A. Wenzl, B.L. Winer, B. R. Yates

Princeton University, Princeton, New Jersey, USA
H. Bouchamaoui, G. Dezoort, P. Elmer, A. Frankenthal, M. Galli, B. Greenberg, N. Haubrich, K. Kennedy, G. Kopp, Y. Lai, D. Lange, A. Loeliger, D. Marlow, I. Ojalvo, J. Olsen, F. Simpson, D. Stickland, C. Tully

University of Puerto Rico, Mayaguez, Puerto Rico, USA
S. Malik, R. Sharma

Purdue University, West Lafayette, Indiana, USA
S. Chandra, R. Chawla, A. Gu, L. Gutay, M. Jones, A.W. Jung, D. Kondratyev, M. Liu, G. Negro, N. Neumeister, G. Paspalaki, S. Piperov, N.R. Saha, J.F. Schulte, F. Wang, A. Wildridge, W. Xie, Y. Yao, Y. Zhong

Purdue University Northwest, Hammond, Indiana, USA
N. Parashar, A. Pathak, E. Shumka

Rice University, Houston, Texas, USA
D. Acosta, A. Agrawal, C. Arbour, T. Carnahan, P. Das, K.M. Ecklund, S. Freed, F.J.M. Geurts, T. Huang, I. Krommydas, N. Lewis, W. Li, J. Lin, O. Miguel Colin, B.P. Padley, R. Redjimi, J. Rotter, M. Wulansatiti, E. Yigitbasi, Y. Zhang

University of Rochester, Rochester, New York, USA
O. Bessidskaia Bylund, A. Bodek, P. de Barbaro[†], R. Demina, A. Garcia-Bellido, H.S. Hare, O. Hindrichs, N. Parmar, P. Parygin[90], H. Seo, R. Taus

Rutgers, The State University of New Jersey, Piscataway, New Jersey, USA
B. Chiarito, J.P. Chou, S.V. Clark, S. Donnelly, D. Gadkari, Y. Gershtein, E. Halkiadakis, C. Houghton, D. Jaroslawski, A. Kobert, S. Konstantinou, I. Laflotte, A. Lath, J. Martins, M. Perez Prada, B. Rand, J. Reichert, P. Saha, S. Salur, S. Schnetzer, S. Somalwar, R. Stone, S.A. Thayil, S. Thomas, J. Vora

University of Tennessee, Knoxville, Tennessee, USA
D. Ally, A.G. Delannoy, S. Fiorendi, J. Harris, T. Holmes, A.R. Kanuganti, N. Karunarathna, J. Lawless, L. Lee, E. Nibigira, B. Skipworth, S. Spanier

Texas A&M University, College Station, Texas, USA
D. Aebi, M. Ahmad, T. Akhter, K. Androsov, A. Bolshov, O. Bouhali[91], A. Cagnotta, V. D'Amante, R. Eusebi, P. Flanagan, J. Gilmore, Y. Guo, T. Kamon, S. Luo, R. Mueller, A. Safonov

Texas Tech University, Lubbock, Texas, USA
N. Akchurin, J. Damgov, Y. Feng, N. Gogate, Y. Kazhykarim, K. Lamichhane, S.W. Lee, C. Madrid, A. Mankel, T. Peltola, I. Volobouev

Vanderbilt University, Nashville, Tennessee, USA
E. Appelt, Y. Chen, S. Greene, A. Gurrola, W. Johns, R. Kunnawalkam Elayavalli, A. Melo, D. Rathjens, F. Romeo, P. Sheldon, S. Tuo, J. Velkovska, J. Viinikainen,

J. Zhang

University of Virginia, Charlottesville, Virginia, USA
B. Cardwell, H. Chung, B. Cox, J. Hakala, G. Hamilton Ilha Machado, R. Hirosky, M. Jose, A. Ledovskoy, C. Mantilla, C. Neu, C. Ramón Álvarez, Z. Wu

Wayne State University, Detroit, Michigan, USA
S. Bhattacharya, P.E. Karchin

University of Wisconsin - Madison, Madison, Wisconsin, USA
A. Aravind, S. Banerjee, K. Black, T. Bose, E. Chavez, S. Dasu, P. Everaerts, C. Galloni, H. He, M. Herndon, A. Herve, C.K. Koraka, S. Lomte, R. Loveless, A. Mallampalli, A. Mohammadi, S. Mondal, T. Nelson, G. Parida, L. Pétré, D. Pinna, A. Savin, V. Shang, V. Sharma, W.H. Smith, D. Teague, H.F. Tsoi, W. Vetens, A. Warden

Authors affiliated with an international laboratory covered by a cooperation agreement with CERN
S. Afanasiev, V. Alexakhin, Yu. Andreev, T. Aushev, D. Budkouski, R. Chistov, M. Danilov, T. Dimova, A. Ershov, S. Gninenko, I. Gorbunov, A. Gribushin, A. Kamenev, V. Karjavine, M. Kirsanov, V. Klyukhin, O. Kodolova[92], V. Korenkov, I. Korsakov, A. Kozyrev, N. Krasnikov, A. Lanev, A. Malakhov, V. Matveev, A. Nikitenko[93,92], V. Palichik, V. Perelygin, S. Petrushanko, S. Polikarpov, O. Radchenko, M. Savina, V. Shalaev, S. Shmatov, S. Shulha, Y. Skovpen, K. Slizhevskiy, V. Smirnov, O. Teryaev, I. Tlisova, A. Toropin, N. Voytishin, A. Zarubin, I. Zhizhin

Authors affiliated with an institute formerly covered by a cooperation agreement with CERN
E. Boos, V. Bunichev, M. Dubinin[83], V. Savrin, A. Snigirev, L. Dudko, V. Kim[23], V. Murzin, V. Oreshkin, D. Sosnov

†: Deceased
[1]Also at Yerevan State University, Yerevan, Armenia
[2]Also at TU Wien, Vienna, Austria
[3]Also at Ghent University, Ghent, Belgium
[4]Also at FACAMP - Faculdades de Campinas, Sao Paulo, Brazil
[5]Also at Universidade do Estado do Rio de Janeiro, Rio de Janeiro, Brazil
[6]Also at Universidade Estadual de Campinas, Campinas, Brazil
[7]Also at Federal University of Rio Grande do Sul, Porto Alegre, Brazil
[8]Also at The University of the State of Amazonas, Manaus, Brazil
[9]Also at University of Chinese Academy of Sciences, Beijing, China
[10]Also at China Center of Advanced Science and Technology, Beijing, China
[11]Also at University of Chinese Academy of Sciences, Beijing, China
[12]Also at School of Physics, Zhengzhou University, Zhengzhou, China
[13]Now at Henan Normal University, Xinxiang, China
[14]Also at University of Shanghai for Science and Technology, Shanghai, China
[15]Now at The University of Iowa, Iowa City, Iowa, USA
[16]Also at Center for High Energy Physics, Peking University, Beijing, China
[17]Also at Zewail City of Science and Technology, Zewail, Egypt
[18]Also at British University in Egypt, Cairo, Egypt
[19]Now at Ain Shams University, Cairo, Egypt
[20]Also at Purdue University, West Lafayette, Indiana, USA

[21]Also at Université de Haute Alsace, Mulhouse, France
[22]Also at Ilia State University, Tbilisi, Georgia
[23]Also at an institute formerly covered by a cooperation agreement with CERN
[24]Also at University of Hamburg, Hamburg, Germany
[25]Also at RWTH Aachen University, III. Physikalisches Institut A, Aachen, Germany
[26]Also at Bergische University Wuppertal (BUW), Wuppertal, Germany
[27]Also at Brandenburg University of Technology, Cottbus, Germany
[28]Also at Forschungszentrum Jülich, Juelich, Germany
[29]Also at CERN, European Organization for Nuclear Research, Geneva, Switzerland
[30]Also at HUN-REN ATOMKI - Institute of Nuclear Research, Debrecen, Hungary
[31]Now at Universitatea Babes-Bolyai - Facultatea de Fizica, Cluj-Napoca, Romania
[32]Also at MTA-ELTE Lendület CMS Particle and Nuclear Physics Group, Eötvös Loránd University, Budapest, Hungary
[33]Also at HUN-REN Wigner Research Centre for Physics, Budapest, Hungary
[34]Also at Physics Department, Faculty of Science, Assiut University, Assiut, Egypt
[35]Also at The University of Kansas, Lawrence, Kansas, USA
[36]Also at Punjab Agricultural University, Ludhiana, India
[37]Also at University of Hyderabad, Hyderabad, India
[38]Also at Indian Institute of Science (IISc), Bangalore, India
[39]Also at University of Visva-Bharati, Santiniketan, India
[40]Also at IIT Bhubaneswar, Bhubaneswar, India
[41]Also at Institute of Physics, Bhubaneswar, India
[42]Also at Deutsches Elektronen-Synchrotron, Hamburg, Germany
[43]Also at Isfahan University of Technology, Isfahan, Iran
[44]Also at Sharif University of Technology, Tehran, Iran
[45]Also at Department of Physics, University of Science and Technology of Mazandaran, Behshahr, Iran
[46]Also at Department of Physics, Faculty of Science, Arak University, ARAK, Iran
[47]Also at Helwan University, Cairo, Egypt
[48]Also at Italian National Agency for New Technologies, Energy and Sustainable Economic Development, Bologna, Italy
[49]Also at Centro Siciliano di Fisica Nucleare e di Struttura Della Materia, Catania, Italy
[50]Also at Università degli Studi Guglielmo Marconi, Roma, Italy
[51]Also at Scuola Superiore Meridionale, Università di Napoli 'Federico II', Napoli, Italy
[52]Also at Fermi National Accelerator Laboratory, Batavia, Illinois, USA
[53]Also at Lulea University of Technology, Lulea, Sweden
[54]Also at Consiglio Nazionale delle Ricerche - Istituto Officina dei Materiali, Perugia, Italy
[55]Also at UPES - University of Petroleum and Energy Studies, Dehradun, India
[56]Also at Institut de Physique des 2 Infinis de Lyon (IP2I), Villeurbanne, France
[57]Also at Department of Applied Physics, Faculty of Science and Technology, Universiti Kebangsaan Malaysia, Bangi, Malaysia
[58]Also at Trincomalee Campus, Eastern University, Sri Lanka, Nilaveli, Sri Lanka
[59]Also at Saegis Campus, Nugegoda, Sri Lanka
[60]Also at National and Kapodistrian University of Athens, Athens, Greece
[61]Also at Ecole Polytechnique Fédérale Lausanne, Lausanne, Switzerland
[62]Also at Universität Zürich, Zurich, Switzerland
[63]Also at Stefan Meyer Institute for Subatomic Physics, Vienna, Austria
[64]Also at Near East University, Research Center of Experimental Health Science, Mersin, Turkey

[65]Also at Konya Technical University, Konya, Turkey
[66]Also at Izmir Bakircay University, Izmir, Turkey
[67]Also at Adiyaman University, Adiyaman, Turkey
[68]Also at Bozok Universitetesi Rektörlügü, Yozgat, Turkey
[69]Also at Istanbul Sabahattin Zaim University, Istanbul, Turkey
[70]Also at Marmara University, Istanbul, Turkey
[71]Also at Milli Savunma University, Istanbul, Turkey
[72]Also at Informatics and Information Security Research Center, Gebze/Kocaeli, Turkey
[73]Also at Kafkas University, Kars, Turkey
[74]Now at Istanbul Okan University, Istanbul, Turkey
[75]Also at Istanbul University - Cerrahpasa, Faculty of Engineering, Istanbul, Turkey
[76]Also at Istinye University, Istanbul, Turkey
[77]Also at Yildiz Technical University, Istanbul, Turkey
[78]Also at School of Physics and Astronomy, University of Southampton, Southampton, United Kingdom
[79]Also at Monash University, Faculty of Science, Clayton, Australia
[80]Also at Università di Torino, Torino, Italy
[81]Also at Karamanoğlu Mehmetbey University, Karaman, Turkey
[82]Also at California Lutheran University;, Thousand Oaks, California, USA
[83]Also at California Institute of Technology, Pasadena, California, USA
[84]Also at United States Naval Academy, Annapolis, Maryland, USA
[85]Also at Bingol University, Bingol, Turkey
[86]Also at Georgian Technical University, Tbilisi, Georgia
[87]Also at Sinop University, Sinop, Turkey
[88]Also at Erciyes University, Kayseri, Turkey
[89]Also at Horia Hulubei National Institute of Physics and Nuclear Engineering (IFIN-HH), Bucharest, Romania
[90]Now at another institute formerly covered by a cooperation agreement with CERN
[91]Also at Hamad Bin Khalifa University (HBKU), Doha, Qatar
[92]Also at Yerevan Physics Institute, Yerevan, Armenia
[93]Also at Imperial College, London, United Kingdom